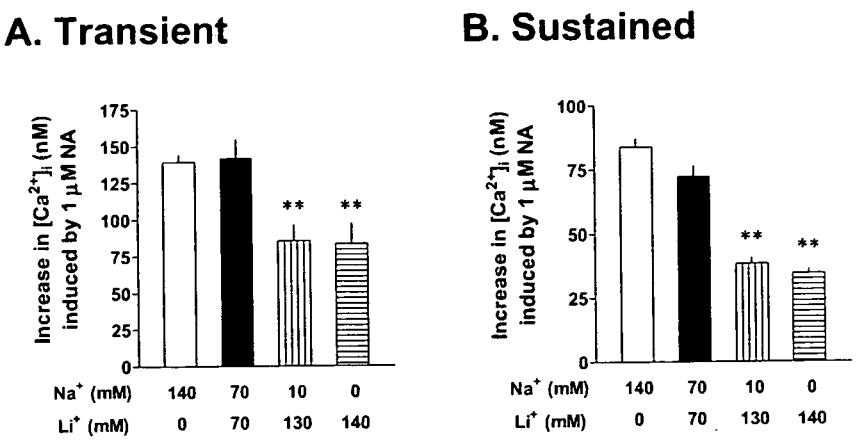

Fig. 3. Effects of reducing extracellular concentrations of Na^+ on the transient (A) and sustained increases (B) in $[Ca^{2+}]_i$ induced by 1 μM NA. The extracellular concentration of Na^+ was reduced by replacing Na^+ with Li^+. Data are presented as means ± S.E.M. of the results obtained from 5 separate experiments. $^{**}P<0.01$: significantly different from the value at 140 mM Na^+.

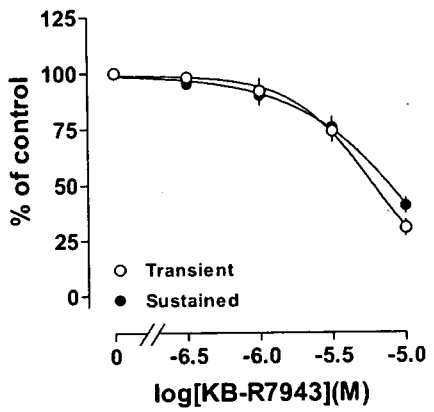

Fig. 4. Inhibitory effects of pretreatment with KB-R7943, an inhibitor of NCX, on the transient and sustained increases in $[Ca^{2+}]_i$ induced by 1 μM NA. The maximum $[Ca^{2+}]_i$ level induced by 1 μM NA for each phase in the presence of 1 mM Ca^{2+} was set to 100% as a control. Data are presented as means ± S.E.M. of the results obtained from 5 separate experiments.

response to NA were insensitive to both inhibitors at concentrations up to 10 μM (data not shown). Therefore, NHE and amiloride-sensitive Na^+ channels do not seem to be major Na^+ entry pathways that contribute to the increase in $[Na^+]_i$.

Involvement of NCX in the NA-induced increases in $[Ca^{2+}]_i$

How is the Na^+ influx associated with the $[Ca^{2+}]_i$ elevation? A potential candidate for such a link is the NCX that mediates Na^+/Ca^{2+} exchange with a ratio of 3 Na^+ : 1 Ca^{2+}, depending on the electrochemical gradient of Na^+ and Ca^{2+} across the plasma membrane. Recently, we have demonstrated that mRNAs for three members of NCX (NCX-1, NCX-2, and NCX-3) were expressed in CHO cells stably expressing ET_AR (16). To determine whether NCX is responsible for the NA-induced $[Ca^{2+}]_i$ increases, therefore, the effect of KB-R7943, an NCX inhibitor (21), was examined. KB-R7943 induced a concentration-dependent inhibition of the transient and sustained $[Ca^{2+}]_i$ increases in response to NA (Fig. 4). The inhibitory effects on the transient and sustained Ca^{2+} responses were 69.6 ± 3.5% and 59.7 ± 3.4%, respectively (n = 5). This result suggests that NCX operating in the reverse mode plays a major role in the NA-induced transient and sustained Ca^{2+} responses.

Pharmacological identification of signaling molecules involved in the transient and sustained increases in $[Ca^{2+}]_i$ induced by NA

To pharmacologically confirm the member(s) of the G proteins involved in the NA-induced transient and sustained increases in $[Ca^{2+}]_i$, the effects of YM-254890, a selective $G_{\alpha q/11}$ inhibitor (22), was examined. In general, α_1-AR is thought to couple with G_q protein in CHO cells (6, 23). As shown in Fig. 5A, YM-254890 suppressed the transient and sustained increases in $[Ca^{2+}]_i$ with different pIC_{50} values (for the transient phase, 6.33 ± 0.08; for the sustained phase, 6.99 ± 0.05, n = 5 for each). The sustained $[Ca^{2+}]_i$ increase was abolished by 0.1 μM YM-254890, which did not affect the transient $[Ca^{2+}]_i$ increase. The inhibitory effect of YM-254890 was about 3-fold more potent for the sustained phase than for the transient phase. These results suggest that NA induces the transient and sustained $[Ca^{2+}]_i$ increases via $G_{\alpha q/11}$.

The principal downstream effector for $G_{\alpha q/11}$ is PLCβ

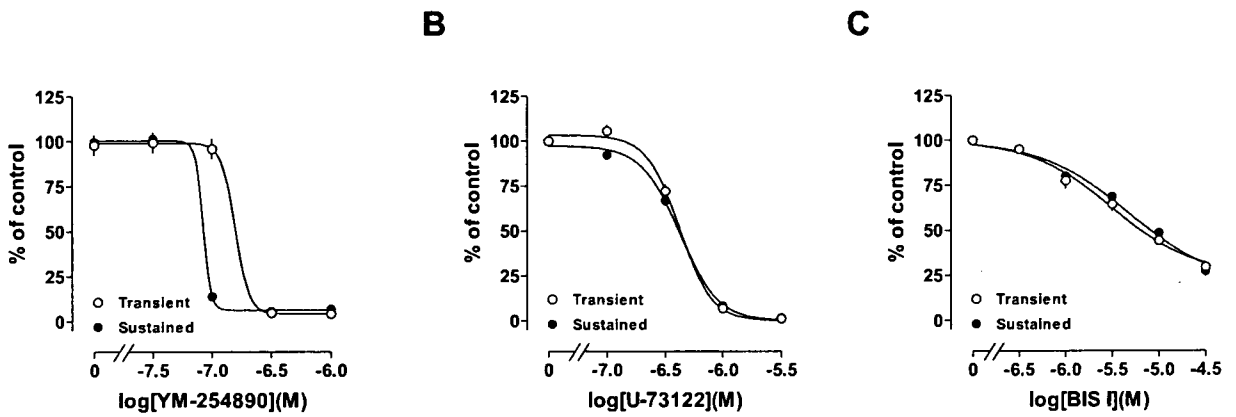

Fig. 5. Inhibitory effects of pretreatment with (A) YM-254890 as a $G_{\alpha q/11}$-selective inhibitor, (B) U-73122 as a PLC inhibitor, and (C) BIS I as a PKC inhibitor on the transient and sustained increases in $[Ca^{2+}]_i$ induced by 1 μM NA. The maximum $[Ca^{2+}]_i$ level induced by 1 μM NA for each phase in the presence of 1 mM Ca^{2+} was set to 100% as a control. Data are presented as means ± S.E.M. of the results obtained from 5 separate experiments.

that cleaves the membrane lipid phosphatidylinositiol-4,5-bisphosphate (PIP_2) into the second messengers IP_3 and DAG, both of which modulate $[Ca^{2+}]_i$ (24). To clarify whether PLCβ is involved in the NA-induced increase in $[Ca^{2+}]_i$, the effects of U-73122, a PLC inhibitor, on the NA-induced $[Ca^{2+}]_i$ responses were examined. As shown in Fig. 3B, U-73122 inhibited the transient and sustained increases in $[Ca^{2+}]_i$ in a concentration-dependent manner (Fig. 5B). These results unequivocally indicate that the Ca^{2+} mobilization activated by NA depends on PLC activation.

DAG, which is the product of PLC activation, can activate the major regulatory kinase PKC. To determine the role of PKC in the NA-induced $[Ca^{2+}]_i$ increase, the effect of BIS I, a PKC inhibitor (25), was examined. Pretreatment with BIS I induced the concentration-dependent inhibition of the transient and sustained increases in $[Ca^{2+}]_i$ (Fig. 5C), indicating that PKC plays an important role in the transient and sustained increases in $[Ca^{2+}]_i$ induced by NA.

Discussion

In the present study, we attempted to determine the mechanisms underlying the NA-induced increases in $[Ca^{2+}]_i$ in CHO cells stably expressing human α_{1A}-AR, focusing on Na^+ influx through ROCs and SOCs. As shown in Fig. 1A, the activation of α_{1A}-AR with NA induced transient and subsequent sustained increases in $[Ca^{2+}]_i$. It is generally thought that the initial Ca^{2+} transient phase produced by $G_{q/11}$ protein-coupled receptors is generated by IP_3-dependent Ca^{2+} release from the intracellular Ca^{2+} store, and the resulting depletion of the Ca^{2+} store triggers the activation of several types of cation channels such as SOC, leading to the sustained $[Ca^{2+}]_i$ increase by initiating extracellular Ca^{2+} entry (26). However, the transient and subsequent sustained Ca^{2+} responses were suppressed following removal of extracellular Ca^{2+}, indicating that Ca^{2+} influx is critical for both of them. Thus, the classic theory is insufficient to account for the initial Ca^{2+} transient increase presented in this study.

We therefore explored the route for the Ca^{2+} entry upon stimulation of α_{1A}-AR expressed in CHO cells. The potential candidates are voltage-independent Ca^{2+} channels such as SOCs and ROCs (designated as non-selective cation channel type 1 and type 2; abbreviated to NSCC-1 and NSCC-2, respectively) rather than VOCCs, because nonexcitable cells including CHO cells ordinarily lack VOCCs (27). In fact, nifedipine, a blocker of L-type VOCC, had no effect on the NA-induced increases in $[Ca^{2+}]_i$ in CHO cells expressing α_{1A}-AR.

To characterize the voltage-independent Ca^{2+} channels involved in the Ca^{2+} responses to NA, we utilized voltage-independent Ca^{2+} channel blockers, SK&F 96365 and LOE 908, which are very useful pharmacological tools for differentiating the three types of Ca^{2+}-permeable channels, SOCs, NSCC-1, and NSCC-2 (17, 28). We have previously demonstrated that NSCC-1 is sensitive to LOE 908, but resistant to SK&F 96365; NSCC-2 is sensitive to both LOE 908 and SK&F 96365; and SOC is resistant to LOE 908, but sensitive to SK&F 96365 (17, 28). In the present study, the NA-induced transient and sustained increases in $[Ca^{2+}]_i$ were inhibited by LOE 908 and SK&F 96365, indicating the involvement of NSCC-2.

Although the contribution of ROCs including NSCC-

2 to the Ca^{2+} entry induced by stimulation of α_{1A}-AR with NA is predictable from a variety of pharmacological and physiological data, the molecular entity of ROCs is unknown. Recently, some studies with molecular and electrophysiological techniques have identified TRPC channels as potential candidates for Ca^{2+}-permeable cation channels, which are operated by the emptying of the intracellular Ca^{2+} store and the second messenger DAG resulting from PLC activation (26, 29). The TRPC family is divided phylogenetically into four distinct subfamilies (TRPC1; TRPC2; TRPC3, 6, and 7; and TRPC4 and 5). Most of these channels are expressed in many types of cells and have been proposed to operate as SOCs and/or ROCs (3). In addition, several reports have shown that a subfamily consisting of TRPC3, 6, and 7 can be blocked by La^{3+} (3). In the present study, La^{3+} inhibited both transient and sustained $[Ca^{2+}]_i$ increases induced by NA, suggesting that the TRPC channel member(s) would contribute to the Ca^{2+} response to NA.

It is well-known that Ca^{2+}-permeable cation channels allow passage of Na^+ as well as Ca^{2+}. An increase in $[Na^+]_i$ is suggested to functionally modify the NCX that couples Na^+ transport to Ca^{2+} transport (2). Indeed, the NA-induced $[Ca^{2+}]_i$ increase was inhibited by reduction of $[Na^+]_e$, as shown in Fig. 3. In addition to cation channels, NHE and amiloride-sensitive Na^+ channels are reported to function as Na^+ influx pathways. However, EIPA, an inhibitor of NHE (13), and amiloride, an inhibitor of the amiloride-sensitive Na^+ channel (20), had no effect on the NA-induced Ca^{2+} response (data not shown). These data indicate that the Na^+ influx following stimulation of α_{1A}-AR with NA is not mediated by NHE or amiloride-sensitive Na^+ channels but probably by Ca^{2+}-permeable cation channels.

To clarify whether the NA-induced $[Ca^{2+}]_i$ increases result from the activation of the NCX reverse mode driven by the increase in $[Na^+]_i$ through NSCC-2, we employed KB-R7943, a NCX inhibitor (30 – 32). KB-R7943 partially inhibited the NA-induced transient and sustained $[Ca^{2+}]_i$ increases. Moreover, we have recently shown that mRNAs for all members of NCX (NCX-1, NCX-2, and NCX-3) are expressed in CHO cells stably expressing ET_AR and that the NCX can operate following stimulation of ET_AR with ET-1 (16). These findings suggest that NCX plays a functional role in the NA-induced transient and sustained increases in $[Ca^{2+}]_i$.

Interestingly, such physiological and functional coupling between NSCC and NCX presented in this study was also observed in HEK293 cells overexpressing TRPC3 where NCX1 can physically associate with TRPC3 to form a Ca^{2+}-signaling complex (33). TRPC3 is suggested to convert PLC-derived signals into local accumulation of Na^+ but not Ca^{2+}, while NCX would function as a Na^+ sensor to convert $[Na^+]_i$ increase into Ca^{2+} signaling (33). Moreover, in rat cardiac myocytes, activation of PLC via G_q protein-coupled angiotensin receptor recruits the TRPC3-NCX1 complex to the plasma membrane to trigger Ca^{2+} influx (34). Taken together, the physiological association of NSCC with NCX in response to the stimulation of $G_{q/11}$ protein-coupled receptors may serve as the regulatory mechanism to maintain Ca^{2+} homeostasis.

Finally, the pharmacological properties of NA-induced $[Ca^{2+}]_i$ increases were characterized using YM-254890 (an inhibitor of $G_{\alpha q/11}$) and U-73122 (an inhibitor of PLC). YM-254890 completely suppressed the NA-induced sustained and transient phases of $[Ca^{2+}]_i$ increases with different potencies. These results indicate that both phases totally depend on $G_{\alpha q/11}$, but the different sensitivity of both phases might be explained as follows: (1) amounts of $G_{q/11}$ protein required for triggering the Ca^{2+} responses differ between both phases, and (2) different members of the $G_{\alpha q/11}$ subfamily are involved in both phases of Ca^{2+} responses.

Furthermore, abolition of both phases of the NA-induced $[Ca^{2+}]_i$ increases by U-73122, an inhibitor of PLC, provides direct evidence that the Ca^{2+} responses to NA in CHO cells expressing α_{1A}-AR are entirely dependent on the $G_{\alpha q/11}$/PLC pathway. On the other hand, a recent report suggested that another G protein, G_{13}, couples with α_{1A}-AR and plays a major role for NA-induced NSCC activation and arachidonic release in CHO cells (35). Taken together, the activation of both $G_{q/11}$ and G_{13} may be required for generation of the Ca^{2+} responses to NA, like ET_AR expressed in CHO cells where both G_q and G_{12} are needed to activate NSCC-2 (17, 28, 36).

In general, activation of $G_{\alpha q/11}$/PLC results in generation of the second messenger DAG that can activate the major regulatory kinase PKC. PKC is reported to modulate the activity of signaling molecules including cation channels and ion transporters. In cardiac cells, PKC activated by ET-1 induces the phosphorylation of the NCX protein (37) and an increase in NCX-mediated outward ionic current as an indicator of reverse mode NCX (38). On the other hand, certain members of the TRPC family are partially inhibited by PKC (2). In the present study, pretreatment with BIS I, a PKC inhibitor (25), partially inhibited the action of NA, suggesting that both phases of the NA-induced $[Ca^{2+}]_i$ increases are mediated by PKC-dependent pathway(s). The action of PKC may be either activation of NCX, inhibition of TRPC channels, or both.

In summary, the present study demonstrated the physiological mechanisms underlying the Ca^{2+} mobiliza-

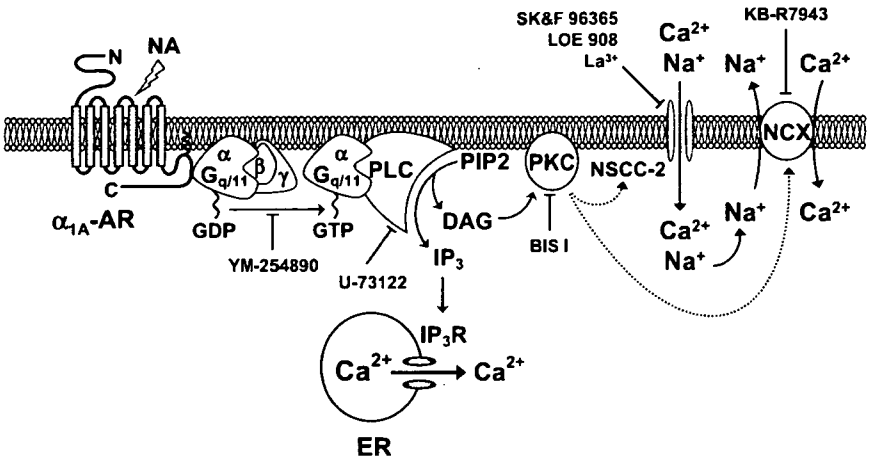

Fig. 6. Possible mechanism involving Ca^{2+} signaling activated by NA in the CHO cells expressing α_{1A}-AR. The application of NA causes $G_{q/11}$ protein-mediated activation of PLC that forms IP_3 and DAG. IP_3R mediating Ca^{2+} release from ER is mainly involved in the transient Ca^{2+} response to NA. In addition, activation of the $G_{q/11}$/PLC pathway elicits facilitation of Ca^{2+} and Na^+ entry via NSCC-2 which belongs to TRPC. PKC activated by DAG is involved in the increase in $[Ca^{2+}]_i$. Speculative mechanisms responsible for the Ca^{2+} responses via PKC are indicated with dotted lines. The increase in $[Na^+]_i$ resulting from Na^+ influx via NSCC-2 eventually triggers Ca^{2+} influx via the NCX operating in the reverse mode.

tion activated by the stimulation of α_{1A}-AR with NA (Fig. 6). The increase in $[Ca^{2+}]_i$ in response to NA in CHO cells expressing α_{1A}-AR results from Ca^{2+} influx via the reverse mode of NCX in exchange for outward Na^+ transport. The operation of NCX in the reverse mode is caused by an increase in $[Na^+]_i$ as a driving force, which is provided by Na^+ influx through NSCC-2 as ROC. NSCC-2 and NCX are activated by α_{1A}-AR through the $G_{\alpha q/11}$/PLC pathway.

Acknowledgments

This study was supported in part by Grant-in-Aids for Young Scientists (B) from the Ministry of Education, Culture, Sports, Science, and Technology (MEXT), Japan (T.H.) and for Scientific Research (B) from Japan Society for the Promotion of Science (JSPS) (S.M.) and by grants from Smoking Research Foundation of Japan (S.M.) and Suzuken Memorial Foundation (T.H.). We thank Dr. Ikunobu Muramatsu (Fukui University) for kindly donating the pCR3 mammalian expression vector containing human α_{1A}-AR cDNA. We also thank Astellas Pharma, Inc. (Tokyo) and Nippon Boehringer Ingelheim Co., Ltd. (Hyogo) for the generously providing YM-254890 and LOE 908, respectively.

References

1 Kawanabe Y, Hashimoto N, Masaki T, Miwa S. Ca^{2+} influx through nonselective cation channels plays an essential role in noradrenaline-induced arachidonic acid release in Chinese hamster ovary cells expressing α_{1A}-, α_{1B}-, or α_{1D}-adrenergic receptors. J Pharmacol Exp Ther. 2001;299:901–907.

2 Spassova MA, Soboloff J, He LP, Hewavitharana T, Xu W, Venkatachalam K, et al. Calcium entry mediated by SOCs and TRP channels: variations and enigma. Biochim Biophys Acta. 2004;1742:9–20.

3 Vazquez G, Wedel BJ, Aziz O, Trebak M, Putney JWJ. The mammalian TRPC cation channels. Biochim Biophys Acta. 2004;1742:21–36.

4 Iwamuro Y, Miwa S, Zhang XF, Minowa T, Enoki T, Okamoto Y, et al. Activation of three types of voltage-independent Ca^{2+} channel in A7r5 cells by endothelin-1 as revealed by a novel Ca^{2+} channel blocker LOE 908. Br J Pharmacol. 1999;126:1107–1114.

5 Yamazaki D, Ohya S, Asai K, Imaizumi Y. Characteristics of the ATP-induced Ca^{2+}-entry pathway in the t-BBEC117 cell line derived from bovine brain endothelial cells. J Pharmacol Sci. 2007;104:103–107.

6 Kawanabe Y, Hashimoto N, Miwa S, Masaki T. Effects of Ca^{2+} influx through nonselective cation channel on noradrenaline-induced mitogenic responses. Eur J Pharmacol. 2002;447:31–36.

7 Inoue R, Okada T, Onoue H, Hara Y, Shimizu S, Naitoh S, et al. The transient receptor potential protein homologue TRP6 is the essential component of vascular α_1-adrenoceptor-activated Ca^{2+}-permeable cation channel. Circ Res. 2001;88:325–332.

8 Berridge MJ, Bootman MD, Roderick HL. Calcium signalling: dynamics, homeostasis and remodelling. Nat Rev Mol Cell Biol. 2003;4:517–529.

9 Parekh AB, Putney JWJ. Store-operated calcium channels. Physiol Rev. 2005;85:757–810.

10 Schaefer M, Plant TD, Obukhov AG, Hofmann T, Gudermann T, Schultz G. Receptor-mediated regulation of the nonselective cation channels TRPC4 and TRPC5. J Biol Chem. 2000;275:17517–17526.

11 Barritt GJ. Receptor-activated Ca^{2+} inflow in animal cells: a

variety of pathways tailored to meet different intracellular Ca^{2+} signalling requirements. Biochem J. 1999;337:153–169.

12 Aiello EA, Villa-Abrille MC, Dulce RA, Cingolani HE, Perez NG. Endothelin-1 stimulates the Na^+/Ca^{2+} exchanger reverse mode through intracellular Na^+ (Na^+_i)-dependent and Na^+_i-independent pathways. Hypertension. 2005;45:288–293.

13 Fujita S, Endoh M. Influence of a Na^+-H^+ exchange inhibitor ethylisopropylamiloride, a Na^+-Ca^{2+} exchange inhibitor KB-R7943 and their combination on the increases in contractility and Ca^{2+} transient induced by angiotensin II in isolated adult rabbit ventricular myocytes. Naunyn Schmiedebergs Arch Pharmacol. 1999;360:575–584.

14 Yang H, Sakurai K, Sugawara H, Watanabe T, Norota I, Endoh M. Role of Na^+/Ca^{2+} exchange in endothelin-1-induced increases in Ca^{2+} transient and contractility in rabbit ventricular myocytes: pharmacological analysis with KB-R7943. Br J Pharmacol. 1999;126:1785–1795.

15 Taniguchi T, Inagaki R, Suzuki F, Muramatsu I. Rapid acid extrusion response triggered by α_1 adrenoceptor in CHO cells. J Physiol. 2001;535:107–113.

16 Horinouchi T, Nishimoto A, Nishiya T, Lu L, Kajita E, Miwa S. Endothelin-1 decreases $[Ca^{2+}]_i$ via Na^+/Ca^{2+} exchanger in CHO cells stably expressing endothelin ET_A receptor. Eur J Pharmacol. 2007;566:28–33.

17 Miwa S, Kawanabe Y, Okamoto Y, Masaki T. Ca^{2+} entry channels involved in endothelin-1-induced contractions of vascular smooth muscle cells. J Smooth Muscle Res. 2005;41:61–75.

18 Wang H, Sakurai K, Endoh M. Pharmacological analysis by HOE642 and KB-R9032 of the role of Na^+/H^+ exchange in the endothelin-1-induced Ca^{2+} signalling in rabbit ventricular myocytes. Br J Pharmacol. 2000;131:638–644.

19 Alvarez dlRD, Canessa CM, Fyfe GK, Zhang P. Structure and regulation of amiloride-sensitive sodium channels. Annu Rev Physiol. 2000;62:573–594.

20 Marunaka Y, Niisato N, Brodovich HO, Eaton DC. Regulation of amiloride-sensitive Na^+-permeable channel by a β_2-adrenergic agonist, cytosolic Ca^{2+} and Cl^- in fetal rat alveolar epithelium. J Physiol. 1999;515:669–683.

21 Amran MS, Homma N, Hashimoto K. Pharmacology of KB-R7943: a Na^+-Ca^{2+} exchange inhibitor. Cardiovasc Drug Rev. 2003;21:255–276.

22 Takasaki J, Saito T, Taniguchi M, Kawasaki T, Moritani Y, Hayashi K, et al. A novel $G_{\alpha q/11}$-selective inhibitor. J Biol Chem. 2004;279:47438–47445.

23 Wu D, Katz A, Lee CH, Simon MI. Activation of phospholipase C by α_1-adrenergic receptors is mediated by the alpha subunits of G_q family. J Biol Chem. 1992;267:25798–25802.

24 Kristiansen K. Molecular mechanisms of ligand binding, signaling, and regulation within the superfamily of G-protein-coupled receptors: molecular modeling and mutagenesis approaches to receptor structure and function. Pharmacol Ther. 2004;103:21–80.

25 Korzick DH, Muller-Delp JM, Dougherty P, Heaps CL, Bowles DK, Krick KK. Exaggerated coronary vasoreactivity to endothelin-1 in aged rats: role of protein kinase C. Cardiovasc Res. 2005;66:384–392.

26 Venkatachalam K, van Rossum DB, Patterson RL, Ma HT, Gill DL. The cellular and molecular basis of store-operated calcium entry. Nat Cell Biol. 2002;4:E263–E272.

27 Perez DM, DeYoung MB, Graham RM. Coupling of expressed α_{1B}- and α_{1D}-adrenergic receptor to multiple signaling pathways is both G protein and cell type specific. Mol Pharmacol. 1993;44:784–795.

28 Kawanabe Y, Okamoto Y, Miwa S, Hashimoto N, Masaki T. Molecular mechanisms for the activation of voltage-independent Ca^{2+} channels by endothelin-1 in Chinese hamster ovary cells stably expressing human $endothelin_A$ receptors. Mol Pharmacol. 2002;62:75–80.

29 Hofmann T, Obukhov AG, Schaefer M, Harteneck C, Gudermann T, Schultz G. Direct activation of human TRPC6 and TRPC3 channels by diacylglycerol. Nature. 1999;397:259–263.

30 Hinata M, Matsuoka I, Iwamoto T, Watanabe Y, Kimura J. Mechanism of Na^+/Ca^{2+} exchanger activation by hydrogen peroxide in guinea-pig ventricular myocytes. J Pharmacol Sci. 2007;103:283–292.

31 Iwamoto T, Shigekawa M. Differential inhibition of Na^+/Ca^{2+} exchanger isoforms by divalent cations and isothiourea derivative. Am J Physiol. 1998;275:C423–C430.

32 Watanabe Y, Koide Y, Kimura J. Topics on the Na^+/Ca^{2+} exchanger: Pharmacological characterization of Na^+/Ca^{2+} exchanger inhibitors. J Pharmacol Sci. 2006;102:7–16.

33 Rosker C, Graziani A, Lukas M, Eder P, Zhu MX, Romanin C, et al. Ca^{2+} signaling by TRPC3 involves Na^+ entry and local coupling to the Na^+/Ca^{2+} exchanger. J Biol Chem. 2004;279:13696–13704.

34 Eder P, Probst D, Rosker C, Poteser M, Wolinski H, Kohlwein SD, et al. Phospholipase C-dependent control of cardiac calcium homeostasis involves a TRPC3-NCX1 signaling complex. Cardiovasc Res. 2007;73:111–119.

35 Kawanabe Y, Hashimoto N, Masaki T. Characterization of G proteins involved in activation of nonselective cation channels and arachidonic acid release by norepinephrine/α_{1A}-adrenergic receptors. Am J Physiol Cell Physiol. 2004;286:C596–C600.

36 Kawanabe Y, Okamoto Y, Nozaki K, Hashimoto N, Miwa S, Masaki T. Molecular mechanism for endothelin-1-induced stress-fiber formation: analysis of G proteins using a mutant $endothelin_A$ receptor. Mol Pharmacol. 2002;61:277–284.

37 Iwamoto T, Pan Y, Wakabayashi S, Imagawa T, Yamanaka H, Shigekawa M. Phosphorylation-dependent regulation of cardiac Na^+/Ca^{2+} exchanger via protein kinase C. J Biol Chem. 1996;271:13609–13615.

38 Zhang YH, James AF, Hancox JC. Regulation by endothelin-1 of Na^+-Ca^{2+} exchange current (I_{NaCa}) from guinea-pig isolated ventricular myocytes. Cell Calcium. 2001;30:351–360.

Journal of Dermatological Science (2007) 47, 151–159

ELSEVIER

Journal of Dermatological SCIENCE

www.intl.elsevierhealth.com/journals/jods

Stimulation of Langerhans cells with ketoprofen plus UVA in murine photocontact dermatitis to ketoprofen

Kenji Atarashi [a,b,*], Kenji Kabashima [a], Katsuhiko Akiyama [b], Yoshiki Tokura [a]

[a] *Department of Dermatology, University of Occupational and Environmental Health, Kitakyushu, Japan*
[b] *Dermal Physiology Team, Fundamental Research Laboratories, Hisamitsu Pharmaceutical Co., Inc., Tsukuba, Japan*

Received 22 January 2007; received in revised form 27 March 2007; accepted 3 April 2007

KEYWORDS
Ketoprofen;
Photocontact dermatitis;
Langerhans cell;
Maturation

Summary

Background: Ketoprofen (KP) clinically evokes the allergic type of photocontact dermatitis when applied to the skin and irradiated with ultraviolet A (UVA). We have established a murine model of photocontact dermatitis to KP, which is a T cell-mediated delayed type hypersensitivity.
Objective: To further explore the mechanism underlying this sensitivity, we investigated whether KP plus UVA activates the antigen-presenting ability of Langerhans cells (LCs).
Methods: We analyzed the expression of surface molecules on LCs in the murine epidermis treated with KP plus UVA by immunohistochemistry and flow cytometry. Changes in the cytokine expression of epidermal cells from KP-phototreated skin were also examined by real-time PCR.
Results: LCs became larger after treatment with KP plus UVA. The number of LCs was significantly decreased 2–3 days after KP phototreatment and recovered on day 5. A flow cytometric analysis revealed that KP plus UVA increased the percentage of LCs that highly expressed MHC class II, CD86, CD80, CD54 and CD40, whereas neither KP nor UVA alone enhanced the expression. KP phototreatment augmented the expression of I-A and CD86 on LCs in KP and UVA dose-dependent manners. A real-time PCR analysis of KP-phototreated skin showed that the expression of mRNA for IL-1α and GM-CSF was immediately increased after treatment.

* Corresponding author at: Dermal Physiology Team, Fundamental Research Laboratories, Hisamitsu Pharmaceutical Co., Inc., 1-25-11 Kannondai, Tsukuba, Ibaraki 305-0856, Japan. Tel.: +81 29 837 2460; fax: +81 29 837 0685.
E-mail address: Kenji_Atarashi@hisamitsu.co.jp (K. Atarashi).

doi:10.1016/j.jdermsci.2007.04.001

Conclusion: A photosensitizing regimen of KP plus UVA activates LCs at least partly by stimulating keratinocytes to produce cytokines. Two strains of mice (BALB/c and AKR) differ in responsiveness to KP and the difference is not related to the activation of keratinocytes.

1. Introduction

Ketoprofen (KP), an arylpropionic acid derivative widely used as a topical anti-inflammatory drug, is clinically well known to induce photocontact dermatitis as an adverse reaction, and ultraviolet A (UVA) is the action spectrum of this photosensitivity [1–7]. In general, photoreactions by photosensitive chemicals are divided into the phototoxic and photoallergic types. While phototoxicity is mediated by active oxygen, especially singlet oxygen [8,9], photoallergy occurs as a consequence of a specific immune reaction mediated by antigen-specific, sensitized T cells [10–14]. KP has both phototoxic and photoallergic potentials, but many clinical observations have indicated that photosensitivity to KP is a photoallergic reaction [1–7].

The two theories, named photohapten and prohapten models, have been put forward to explain the formation of photoallergen [11,14]. According to the photohapten theory, photosensitizing chemicals and protein need to coexist upon exposure to UVA in a noncovalent manner, and UVA turns it covalent [11,14]. On the other hand, the prohapten theory suggests that UVA simply converts photosensitizing substances into ordinary hapten, which subsequently binds to protein. It seems that most of photoallergic substances have a photohaptenic moiety, as typically demonstrated in 3,3′,4′,5-tetrachlorosalicylanilide (TCSA) [15–18], quinolones [10–12], and afloqualone [13]. KP serves as a photohapten because of its photocoupling ability to protein [19]. Our study has suggested that photohaptens bind to self-peptides located in the groove of major histocompatibility complex (MHC) molecules of antigen-presenting cells [20].

In photocontact dermatitis, epidermal Langerhans cells (LCs) serve as photoantigen-presenting cells and transport a given photoantigen to the draining lymph nodes where they present it to photoantigen-specific T cells. Upon stimulation with an ordinary hapten, LCs are matured to highly express MHC class II molecules [21]. Not only MHC class II molecules but also costimulatory molecules such as CD86 and CD80 and adhesion molecules such as CD54 and CD40 play in important roles on the antigen-presentation [22–25]. Likewise, representative photohapten TCSA [26,27] plus UVA augments the expression of MHC class II, CD86, CD80 and CD54 on LCs [16]. It is well known that keratinocyte-derived granulocyte/macrophage colony stimulating factor (GM-CSF), interleukin (IL)-1α and tumor necrosis factor (TNF)-α are essential for the viability of LCs, and upregulate the antigen-presenting activity of LCs [23,28–30]. Thus, it is possible that photohapten plus UVA exerts the LC-stimulating action by stimulating keratinocytes to produce these cytokines.

We have previously established a murine model of photocontact dermatitis to KP [31]. Mice bearing H-2^k such as AKR are high responders, whereas H-2^d mice such as BALB/c mice are low responders in this sensitivity [31]. This is in contrast to photocontact dermatitis to TCSA, in which H-2^d and H-2^k mice are high and low responders, respectively [15,17]. KP photosensitivity is mediated by T cells, and both $CD4^+$ and $CD8^+$ T cells are required for the full blown sensitivity [31]. Th2 cytokines/chemokines as well as Th1 cytokines/chemokines are expressed in the lymph nodes and epidermis of challenged mice. In this study, we investigated alterations in the morphology, cell number, and surface molecule expression of LCs treated with KP plus UVA. Keratinocyte-derived LC-supportive cytokines were also examined. Results suggest that KP plus UVA play an immunostimulatory role for these cells in the mouse strain highly responsive to KP phototreatment.

2. Materials and methods

2.1. Chemicals and monoclonal antibodies (mAbs)

Ketoprofen (KP) was obtained from Hisamitsu Pharmaceutical Co., Inc. (Tokyo, Japan) and TCSA was purchased from Kanto Chemical Co., Inc. (Tokyo, Japan). Anti-Fcγ II/III receptor (2.4G2) monoclonal antibody (mAb), phycoerythrin (PE)-labeled anti-mouse I-A^d (AMS-32.1) and I-A^k (11–5.2) mAbs, and fluorescein isothiocyanate (FITC)-labeled anti-mouse CD86 (GL1), CD80 (16-10A1), CD54 (3E2), CD40 (3/23) mAbs and isotype matched immunoglobulins (Igs) were purchased from BD Pharmingen (San Diego, CA).

2.2. Mice

AKR (H-2^k) and BALB/c (H-2^d) mice were obtained from Kyudo Co., Ltd. (Kumamoto, Japan). Female mice, 8–10 weeks old, were used unless otherwise mentioned.

2.3. Treatment of earlobes with KP plus UVA

As UVA source, black light (FL20SBL-B) emitting UVA ranging from 320 to 400 nm with a peak emission at 365 nm was purchased from Toshiba Electric Co. (Tokyo, Japan). With a UV radiometer (Topcon Technohouse Corp., Tokyo, Japan), the energy output of three 20-W tubes of black light at a distance of 20 cm was 1.8 mW/cm^2 at 365 nm. Irradiation was performed through a pane of 3 mm thickness glass. Both sides of each earlobe of mice were painted with 10 μl of KP in ethanol and irradiated with UVA. Unless otherwise mentioned, 20 or 10% KP and 32 J/cm^2 UVA were used.

2.4. LC enumeration in epidermal sheets

Epidermal sheets were separated from dermis with 0.5 M ammonium thiocyanate, fixed in acetone for 5 min at −20 °C, and stained with biotinated anti-I-A^d mAb at a final concentration of 4 μg/ml for 18 h at 4 °C, and then with Cy3-streptavidin at a final concentration of 2 μg/ml for 2 h at 37 °C. Stained LCs were enumerated in two random visual field at 200× magnification in two different sections and were expressed as cells/mm^2.

2.5. Preparation of epidermal cell suspensions and enrichment of LCs

The procedure was previously described [12,32]. Briefly, cartilage-removed skin sheets from earlobes were floated in 0.2% trypsin in phosphate buffered saline (PBS; pH 7.4) for 1 h at 37 °C. Epidermis was then separated from dermis with forceps in PBS supplemented with 10% fetal calf serum (FCS). Epidermal cell suspensions were prepared by vigorous pipetting and filtration through nylon mesh. For enrichment of LCs, freshly isolated single cell suspensions of epidermal cells were centrifuged over a Ficoll-Hypaque gradient and interface cells were collected.

2.6. Flow cytometry

All mAbs were used at 1–5 μg/10^6 cells, and each incubation was performed for 30 min at 4 °C, followed by two washes in PBS supplemented with 5% FCS and 0.02% sodium azide. LC-enriched epidermal cells were preincubated with 2.4G2 for 5 min to prevent non-specific binding of the subsequent reagents to Fc receptors and stained with anti-I-A^k mAb in AKR mice or anti-I-A^d mAb in BALB/c mice and anti-CD86, -CD80, -CD54 or -CD40 mAb. Fluorescence profiles were analyzed in a FACScalibur (Becton Dickinson, Franklin Lakes, NJ). LCs were identified with the expression of MHC class II and cell size. Viable cells were identified by 7-AAD uptake. The mean fluorescence intensity (MFI) was calculated by using CellQuest, which is an operating software for a FACScalibur. The relative MFI was calculated with the ratio to each control.

2.7. Quantitative RT-PCR

Total mRNA was extracted from epidermal cell suspensions with the SVTotal RNA Isolation system (Promega, Madison, WI) according to the manufacturer's protocol. Target gene expression was quantified in a two-step RT-PCR. cDNA was reverse transcribed from total RNA samples using the TaqMan RT reagents (Applied Biosystems, Foster City, CA). Murine IL-1α (Assay ID: Mm00439620_m1) and GM-CSF (Assay ID: Mm00438328_m1) expression was quantified using TaqMan Gene Expression Assay (Applied Biosystems) in the ABI PRISM 7000 sequence detection system (Applied Biosystems). As an endogenous reference for these PCR quantification studies, GAPDH gene expression was measured using the TaqMan rodent GAPDH control reagents (Applied Biosystems). The relative expression was calculated using the $2^{-\Delta\Delta C_T}$ method [33]. The expression of the target gene normalized to an endogenous reference and relative to calibrator is given by the formula $2^{-\Delta\Delta C_T}$. Gene expression in untreated mice was used as a calibrator expression to calculate $\Delta\Delta C_T$.

2.8. Photocontact dermatitis to KP and TCSA

The procedures for induction and elicitation of photocontact dermatitis to KP [31] and TCSA [15] were reported previously. Briefly, for KP photosensitivity, mice were sensitized on days 0 and 1 by painting with 50 μl of 4% KP in acetone and subsequent irradiation with 20 J/cm^2 UVA on the shaved abdomen, and challenged on day 5 with 25 μl of 2% KP in ethanol plus 20 J/cm^2 UVA on each earlobe. For TCSA photosensitivity, mice were sensitized with 50 μl of 1% TCSA in acetone plus 12 J/cm^2 UVA on day 0 and 1 and challenged on day 5 with 20 μl of 0.1% TCSA in ethanol plus 20 J/cm^2 UVA. The ear swelling responses were measured before and after

sensitization with a dial thickness gauge. Data were expressed as Δ ear thickness.

2.9. Statistical analysis

The *P* values were calculated using Dunnett type multiple comparison, Student's *t*-test or Paired *t*-test. Values ≤ 0.05 were considered significant.

3. Results

3.1. Morphological and numerical changes of LCs in KP-phototreated skin

The dorsal aspect of murine earlobes were painted with 5 μl of 20% KP in ethanol and irradiated with 32 J/cm^2 UVA. Epidermal sheets were obtained from earlobes 1, 2, 3 or 5 days after KP phototreatment and stained with anti-I-A^d mAb. As typically observed on day 2, LCs in the epidermis treated with KP plus UVA were stained brightly for MHC class II molecules (Fig. 1). They became larger and maintained well-developed dendritic configuration. This morphological alteration was virtually the same as that seen in LCs phototreated with TCSA, a representative photohapten [16]. There was no change in LCs treated with KP or UVA alone. Thus, both KP and UVA were necessary for stimulation of LCs.

The numerical change was assessed in the epidermal sheets. When earlobes were phototreated with KP at 20%, the number of MHC class II$^+$ cells was unchanged on day 1, significantly decreased on days 2 and 3, and recovered on day 5 (Fig. 2). The comparable change was observed in LCs phototreated with 0.2% TCSA.

3.2. Enhanced expression of MHC class II and other surface molecules on LCs by KP phototreatment

The expression levels of MHC class II and costimulatory molecules on LCs were examined in earlobes painted with 10 μl of 10% KP in ethanol and irradiated with 32 J/cm^2 UVA. LC-enriched epidermal cell suspensions were prepared from earlobes 18 h after KP phototreatment, and the expression of each molecule was analyzed by flow cytometry. Immature LCs express a high level of MHC class II and low levels of CD86, CD80, CD54 and CD40 molecules. Upon maturation, the expression of all the molecules is upregulated [21–25]. Fig. 3A shows representative data gated for I-A$^+$ cells so that only LCs were analyzed. The stimulation level of LCs was

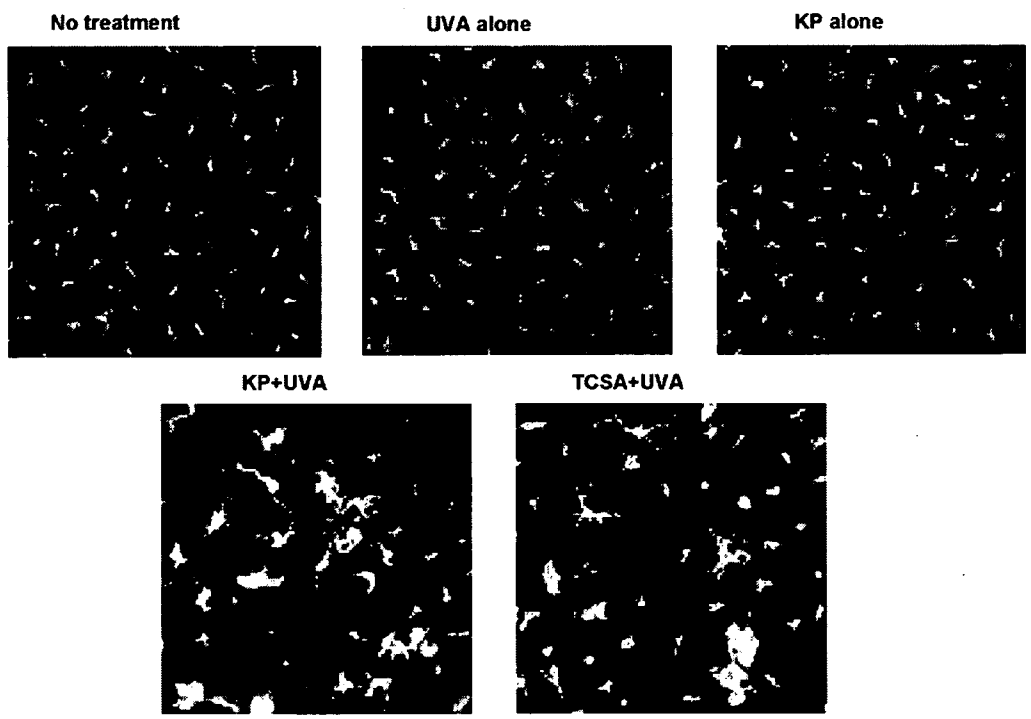

Fig. 1 Morphological change of epidermal MHC class II$^+$ LCs from KP-phototreated skin. Epidermal sheet from earlobes non-treated or treated with UVA alone, 20% KP alone, 20% KP plus 32 J/cm^2 of UVA, or TCSA plus 32 J/cm^2 of UVA were stained with anti-I-A^d and analyzed by fluorescent microscopy. Data indicate representative images of epidermal I-A^{d+} LC ($n = 4$ or 6). In all photographs, the original magnification is 200×.

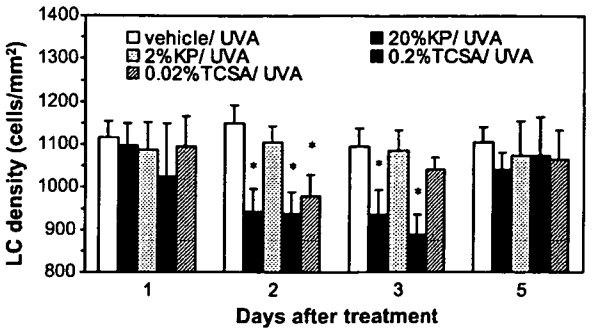

Fig. 2 Decreased density of LCs in epidermis treated with KP plus UVA. Epidermal sheets from earlobes treated with vehicle plus 32 J/cm^2 of UVA, 20% KP plus 32 J/cm^2 of UVA, 2% KP plus 32 J/cm^2 of UVA, 0.2% TCSA plus 32 J/cm^2 of UVA, or 0.02% TCSA plus 32 J/cm^2 of UVA were stained with anti-I-A^d and analyzed by fluorescent microscopy. The positively stained LCs were enumerated in two random visual field at 200× magnification in two different sections and were expressed as cells/mm^2. Statistical analysis was performed with Dunnett type multiple comparison. *$p < 0.05$ vs. vehicle plus UVA.

expressed as the percentage of I-A-highly positive and CD86-positive population. LCs from mice untreated, or treated with KP or UVA alone contained no substantial number of the activated cells. Treatment with KP plus UVA increased the percentage of activated LCs, similarly to TCSA phototreatment, but at a lower level. Thus, both KP and UVA were required for the augmentation of MHC class II and CD86 expression on LCs.

In addition to I-A and CD86, CD80, CD40 and CD54 were also examined. The percentages of LCs expressing these molecules were increased by KP plus UVA, but the numbers of positive cells were fewer than that of I-A$^+$CD86$^+$ cells (Fig. 3B). Again, the levels of upregulation were lower than TCSA phototreatment. Moreover, the data with isotype matched controls indicated no interference by a non-specific binding of Igs in any treatment.

Earlobes of mice were treated with 0.4, 2 or 10% KP in combination with 32 J/cm^2 UVA (Fig. 4A). Alternatively, earlobes painted with 4% KP were irradiated at 0, 8, 16, 32 or 64 J/cm^2 of UVA (Fig. 4B). The expression of both MHC class II and CD86 on LCs was elevated in dose-dependent manners up to the amounts monitored.

3.3. Differences in the MHC class II and CD86 expression induced by KP or TCSA phototreatment between AKR and BALB/c mice

As represented by Fig. 5A and B, in murine photocontact dermatitis, AKR mice are high responders for KP and low responders for TCSA, whereas BALB/c mice are high for TCSA and low for KP [15,31]. In particular, the low responsiveness of AKR mice to TCSA is intriguing. Therefore, we investigated differences in the augmented expression of MHC class II and CD86 by phototreatment with KP or TCSA between AKR and BALB/c mice. The two strains of mice were painted with 10 μl of 10% KP or 0.2% TCSA in ethanol on earlobes and irradiated with 32 J/cm^2 of UVA. Although differences between AKR and BALB/c in the expression of MHC class II and CD86 by KP phototreatment was not statistically significant, AKR mice tended to exhibit slightly high expression of these molecules as compared to BALB/c mice in the independent individual experiments. In TCSA phototreatment, BALB/c mice showed significantly higher expression of these molecules than did AKR mice. These results suggested that each photohapten has different photostimulatory ability for LCs, depending on the mouse strain, and the magnitude of photocontact dermatitis is associated with the levels of MHC class II and costimulatory molecules.

3.4. Enhanced expression of IL-1α and GM-CSF in keratinocytes treated with KP plus UVA

Total RNA was extracted from epidermal cells of earlobes phototreated with KP and subjected to real-time PCR for keratinocyte-derived cytokines, IL-1α, and GM-CSF. Earlobes were taken from mice immediately (0 h) or 12 h after cessation of UVA irradiation. The relative quantity of GM-CSF was remarkably increased at 0 h and decreased to the untreated level at 12 h (Fig. 6). IL-1α expression of KP-phototreated skin was upregulated, but to a lesser degree of TCSA phototreatment. Treatment with KP or UVA alone was not stimulatory.

4. Discussion

We have previously shown that photocontact dermatitis to KP is induced in mice and mediated by T cells [31]. Our present study was conducted to investigate the early sensitization event in this sensitivity, focusing on KP-induced alterations in LCs. We demonstrated that KP plus UVA, but not KP or UVA alone, induces morphological changes of epidermal LCs and stimulates them to express MHC class II, CD86, CD80, CD54 and CD40 molecules, indicating that KP phototreatment maturates LCs. Moreover, LC density in the epidermal sheets was decreased by KP phototreatment. In our murine model of photocontact dermatitis to KP, we used

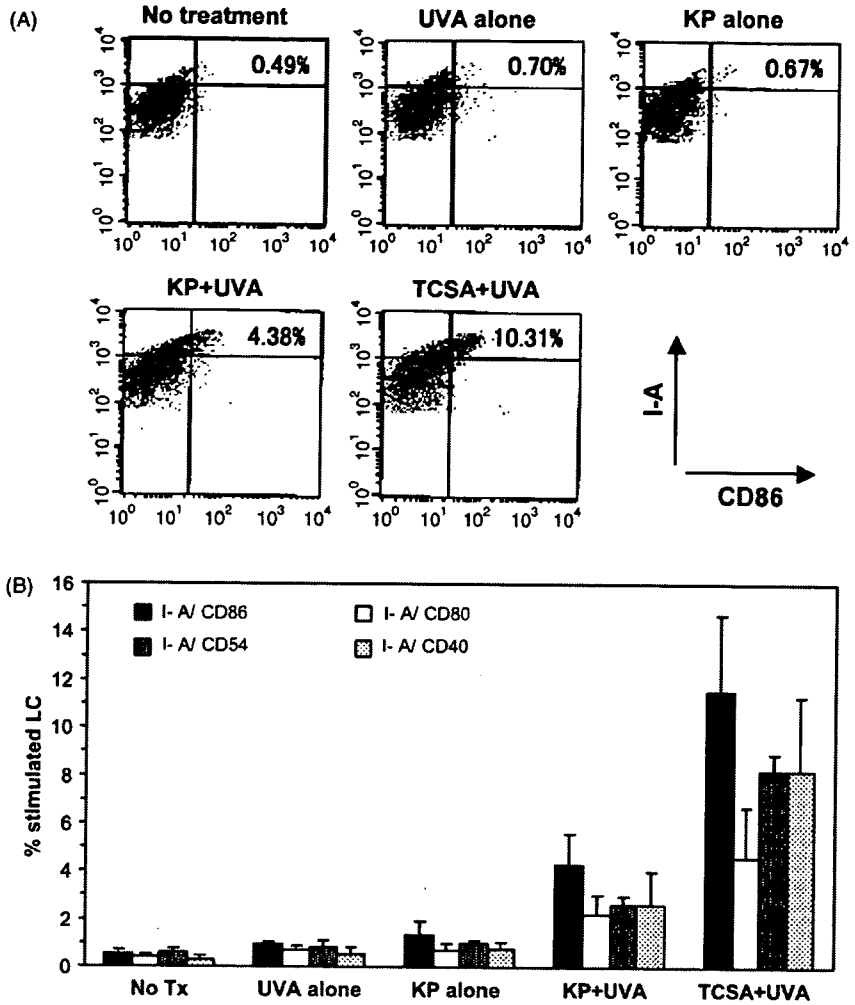

Fig. 3 Augmented expression of MHC class II, CD86, CD80, CD54 and CD40 on LCs in epidermis treated with KP and UVA. LC-enriched epidermal cells from earlobes non-treated, or 32 J/cm^2 of UVA alone, 10% KP alone, 10% KP plus 32 J/cm^2 of UVA, or 0.2% TCSA plus 32 J/cm^2 of UVA were double-stained with anti-I-A^d and anti-CD86, -CD80, -CD54, or —CD40 mAbs and analyzed by flow cytometry. (A) Data indicate representative dot-plots of LCs stained with anti-I-A^d and anti-CD86 mAbs. Percent in each dot-plot indicates the rate of I-A^{d++} and CD86$^+$ stimulated LC. (B) Data indicate mean values of I-A^{d++} and CD86$^+$, CD80$^+$, CD54$^+$, or CD40$^+$ stimulated LCs (n = 4 or 5). The error bars represent S.D.

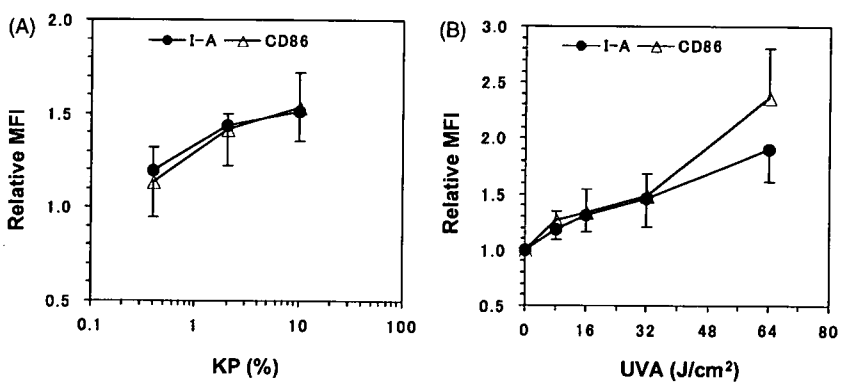

Fig. 4 Dose dependent augmentation of MHC class II and CD86 expression on LCs by KP and UVA. Mice were treated with various concentrations of KP plus 32 J/cm^2 of UVA (A) or 4% KP plus various doses of UVA (B). LC-enriched epidermal cells from earlobes were double-stained with anti-I-A^d and anti-CD86 mAbs and analyzed by flow cytometry. Data indicate the expression of MHC class II (closed circle) and CD86 (open triangle). Relative MFI values were calculated to individual control of 0% KP plus 32 J/cm^2 of UVA (A, n = 3) or 4% KP plus 0 J/cm^2 of UVA (B, n = 3). The error bars represent S.D.

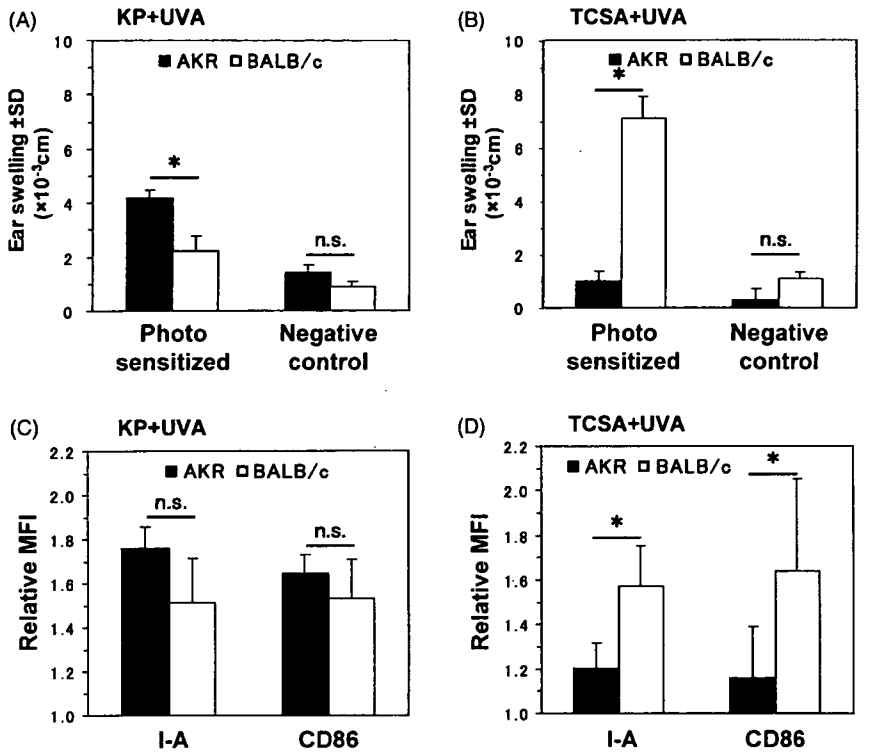

Fig. 5 Comparison between AKR and BALB/c mice in susceptibility of LC expression of MHC class II and CD86 to KP plus UVA. (A and B) AKR (closed column) and BALB/c (open column) mice were photosensitized with 4% KP (A) or 1% TCSA (B) and photochallenged with 2% KP (A) or 0.1% TCSA (B). The ear swelling responses were measured ($n = 4$–6). Statistical analysis was performed with Student's t-test. $^*p < 0.05$. (C and D) LC-enriched epidermal cells from earlobes non-treated or treated with 10% KP plus 32 J/cm^2 of UVA (C) or 0.2% TCSA plus 32 J/cm^2 of UVA (D) were double-stained with anti-I-A^d and anti-CD86 mAbs and analyzed by flow cytometry. Relative MFI values were calculated to individual non-treatment control ($n = 3$). Data indicate augmentation of MHC class II and CD86 expression in AKR (closed column) and BALB/c (open column) mice. The error bars represent S.D. Statistical analysis was performed with Paired t-test. $^*p < 0.05$.

4% in 50 μl solution and 2% KP in 25 μl solution for sensitization and challenge, respectively. In the present LC morphology and number studies, the alterations were obtained with 20%, but not 2%, KP in 5 μl solution. This raises the possibility that the total applied amount of KP determines the response. Alternatively, some antigen-presenting cells other than LCs, such as dermal dendritic cells, might play a role for sensitization and elicitation of photocontact dermatitis. Compared to ordinary contact hypersensitivity, however, UVA irradiation is required for sensitization and challenge, and therefore, dermal dendritic cells seem to be less photomodified with KP than LCs. The role of such antigen-presenting cells is an issue to be elucidated. There are two possibilities in the reduction of LC number. One is that LCs undergoing maturation migrate to the draining lymph nodes, as previously documented in ordinary haptens [34,35]. The other possibility remains that KP exerts phototoxic action to LCs. Considering that we analyzed only viable LCs with high CD86 expression in our flow cytometry study, the phototoxic effect is minimal in this reduction, and the migration mechanism is more likely.

The ability of KP phototreatment to maturate LCs was not so high as that of TCSA phototreatment. This suggests that KP photoproducts are formed to a lesser degree than TCSA photoproducts, or the photoantigenicity of KP is weaker than TCSA. Alternatively, KP possibly affects LC maturation by its pharmacological action of nonsteroidal anti-inflammatory drug. Contact sensitization of the skin with a hapten stimulates keratinocytes to release prostaglandin E2 (PGE2), which promotes LC migration to lymph nodes [36]. We found that KP suppresses the production of PGE2 by murine keratinocytes (unpublished observation).

It is well known that keratinocytes release many cytokines, some of which play a supportive role for LCs. GM-CSF is essential for maintenance of LC viability and upregulation of LC function [23,28–30]. IL-1α upregulates LC function in the presence of GM-CSF [29,30]. TNF-α also plays an important role in the viability and migration of LCs [23,30]. In the present study, keratinocytes were stimulated to

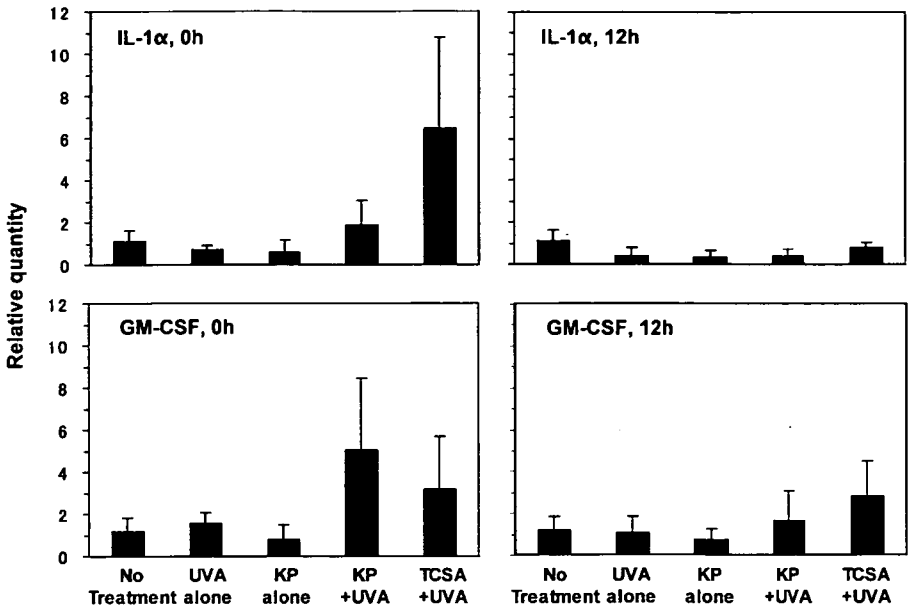

Fig. 6 Augmented expression of cytokine mRNA in epidermal cells. Total mRNA was extracted from epidermal cells from earlobes of non-treated or treated with 32 J/cm^2 of UVA alone, 10% KP alone, 10% KP plus 32 J/cm^2 of UVA, or 0.2% TCSA plus 32 J/cm^2 of UVA. Murine IL-1α, GM-CSF and TNF-α gene expression were quantified in a two-step RT-PCR using TaqMan probes. GAPDH gene expression was measured as an endogenous control. Results represent normalized mean target mRNA amounts relative to non-treated mice using the $\Delta\Delta C_T$ method ($n = 4$ or 5). The error bars represent S.D.

produce IL-1α and GM-CSF by KP plus UVA, suggesting that LC maturation is mediated at least by these kertinocyte-derived cytokines.

In murine photocontact dermatitis, the magnitude of response depends on the strain of mice. In KP photocontact dermatitis, the responses of H-2^k stains, such as AKR, are higher than those of H-2^d strains, such as BALB/c [31]. On the other hands, H-2^d mice exhibit remarkably high responses in TCSA photocontact dermatitis, whereas H-2^k mice are low responders in this sensitivity [15]. Thus, the sensitivity seems to be controlled by MHC class II molecules. In this study, the augmented expression of MHC class II and CD86 was in accordance with the magnitude of KP or TCSA photocontact dermatitis in AKR and BALB/c mice. We further examined the difference in mRNA expression for IL-1α and GM-CSF by epidermal cells between BALB/c and AKR mice phototreated with KP or TCSA. However, the cytokine expression of AKR mice was higher than that of BALB/c in not only KP but also TCSA phototreatment (data not shown). Thus, the difference in LC maturation and resultant sensitivity magnitude is not attributable to keratinocyte cytokine production.

Our study suggests two clinically important notions. First, nonsteroidal anti-inflammatory drugs are capable of functioning as photohapten, thereby stimulating LCs to mature. In this process, keratinocytes are also stimulated to produce LC-stimulatory cytokines. Second, there are differences among individuals in the susceptibility of LC responses to photohaptenic drugs upon UVA exposure. A number of reports have documented patients with severe photocontact dermatitis to KP [1,2,4]. In such cases, a predisposition to the photosensitivity might be closely associated with MHC haplotype.

References

[1] Cusano F, Rafenelli A, Bacchilega R, Errico G. Photo-contact dermatitis from ketoprofen. Contact Dermatitis 1987;17:108–9.

[2] Nabeya RT, Kojima T, Fujita M. Photocontact dermatitis from ketoprofen with an unusual clinical feature. Contact Dermatitis 1995;32:52–3.

[3] Le Coz CJ, Bottlaender A, Scrivener JN, Santinelli F, Cribier BJ, Heid E, et al. Photocontact dermatitis from ketoprofen and tiaprofenic acid: cross-reactivity study in 12 consecutive patients. Contact Dermatitis 1998;38:245–52.

[4] Sugiura M, Hayakawa R, Kato Y, Sugiura K, Ueda H. 4 cases of photocontact dermatitis due to ketoprofen. Contact Dermatitis 2000;43:16–9.

[5] Matsushita T, Kamide R. Five cases of photocontact dermatitis due to topical ketoprofen: photopatch testing and cross-reaction study. Photodermatol Photoimmunol Photomed 2001;17:26–31.

[6] Mozzanica N, Pigatto PD. Contact and photocontact allergy to ketoprofen: clinical and experimental study. Contact Dermatitis 1990;23:336–40.

[7] Sugiura M, Hayakawa R, Xie Z, Sugiura K, Hiramoto K, Shamoto M. Experimental study on phototoxicity and the

photosensitization potential of ketoprofen, suprofen, tiaprofenic acid and benzophenone and the photocross-reactivity in guinea pigs. Photodermatol Photoimmunol Photomed 2002;18:82–9.
[8] Iwamoto Y, Mifuchi I, Yielding LW. Photodynamic deoxyribonucleic acid strand breaking activities of enoxacin and afloqualone. Chem Pharm Bull 1992;40:1868–70.
[9] Hashizume H, Tokura Y, Oku T, Iwamoto Y, Takigawa M, Photodynamic. DNA-breaking activity of serum from patients with various photosensitivity dermatoses. Arch Dermatol Res 1995;287:586–90.
[10] Tokura Y. Quinolone photoallergy: photosensitivity dermatitis induced by systemic administration of photohaptenic drugs. J Dermatol Sci 1998;18:1–10.
[11] Tokura Y, Nishijima T, Yagi H, Furukawa F, Takigawa M. Photohaptenic properties of fluoroquinolones. Photochem Photobiol 1996;64:838–44.
[12] Tokura Y, Seo N, Yagi H, Furukawa F, Takigawa M. Cross-reactivity inmurine fluoroquinolone photoallergy: exclusive usage of TCR Vβ 13 by immune T cells that recognize fluoroquinolone-photomodified cells. J Immunol 1998;160: 3719–28.
[13] Tokura Y, Ogai M, Yagi H, Takigawa M. Afloqualone photosensitivity: immunogenicity of afloqualone-photomodified epidermal cells. Photochem Photobiol 1994;60:262–7.
[14] Tokura Y. Immune responses to photohaptens: implications for the mechanisms of photosensitivity to exogenous agents. J Dermatol Sci 2000;23:S6–9.
[15] Tokura Y, Satoh T, Takigawa M, Yamada M. Genetic control of contact photosensitivity to tetrachlorosalicylanilide. I. Preferential activation of suppressor T cells in low responder H-2k mice. J Invest Dermatol 1990;94:471–6.
[16] Nishijima T, Tokura Y, Imokawa G, Takigawa M. Photohapten TCSA painting plus UVA irradiation of murine skin augments the expression of MHC class II molecules and CD86 on Langerhans cells. J Dermatol Sci 1999;19:202–7.
[17] Suzuki K, Yamazaki S, Tokura Y. Expression of T-cell cytokines in challenged skin of murine allergic contact photosensitivity: low responsiveness is associated with induction of Th2 cytokines. J Dermatol Sci 2000;23:138–44.
[18] Gerberick GF, Ryan CA, Fletcher ER, Howard AD, Robinson MK. Increased number of dendritic cells in draining lymph nodes accompanies the generation of contact photosensitivity. J Invest Dermatol 1991;96:355–61.
[19] Lahoz A, Hernandez D, Miranda MA, Perez-Prieto J, Morera IM, Castell JV. Antibodies directed to drug epitopes to investigate the structure of drug-protein photoadducts. Recognition of a common photobound substructure in tiaprofenic acid/ketoprofen cross-photoreactivity. Chem Res Toxicol 2001;14:1486–91.
[20] Tokura Y, Seo N, Fujie M, Takigawa M. Quinolone-photoconjugated major histocompatibility complex class II-binding peptides with lysine are antigenic for T cells mediating murine quinolone photoallergy. J Invest Dermatol 2001;117:1206–11.
[21] Aiba S, Katz SI. Phenotypic and functional characteristics of in vivo-activated Langerhans cells. J Immunol 1990;145: 2791–6.
[22] Rattis FM, Peguet-Navarro J, Staquet MJ, Dezutter-Dambuyant C, Courtellemont P, Redziniak G, et al. Expression and function of B7-1 (CD80) and B7-2 (CD86) on human epidermal Langerhans cells. Eur J Immunol 1996;26:449–53.
[23] Chang CH, Furue M, Tamaki K. B7-1 expression of Langerhans cells is up-regulated by proinflammatory cytokines, and is down-regulated by interferon-gamma or by interleukin-10. Eur J Immunol 1995;25:394–8.
[24] Peguet-Navarro J, Dalbiez-Gauthier C, Rattis FM, Van Kooten C, Banchereau J, Schmitt D. Functional expression of CD40 antigen on human epidermal Langerhans cells. J Immunol 1995;155:4241–7.
[25] Salgado CG, Nakamura K, Sugaya M, Toda Y, Asahina A, Fukuoka S. Differential effects of cytokines and immunosuppressive drugs on CD40, B7-1 and B7-2 expression on purified epidermal Langerhans cells. J Invest Dermatol 1999;113:1021–7.
[26] Harber LC, Harris H, Baer RL. Photoallergic contact dermatitis due to halogenated salicylanilides and related compounds. Arch Dermatol 1966;94:255–62.
[27] Epstein JH, Wuepper KD, Maibach HI. Photocontact dermatitis to halogenated salicylanilides and related compounds: a clinical and histological review of 26 patients. Arch Dermatol 1968;97:236–44.
[28] Witmer-Pack MD, Oliver W, Valinsky J, Schuler G, Steinman RM. Granulocyte/macrophage colony-stimulating factor is essential for the viability and function of cultured murine epidermal Langerhans cells. J Exp Med 1987;166:1484–98.
[29] Heufler C, Koch F, Schuler G. Granulocyte/macrophage colony-stimulating factor and interleukin 1 mediate the maturation of murine epidermal Langerhans cells into potent immunostimulatory dendritic cells. J Exp Med 1988;167:700–5.
[30] Nakae S, Naruse-Nakajima C, Sudo K, Horai R, Asano M, Iwamoto Y. IL-1 alpha, but not IL-1 beta, is required for contact-allergen-specific T cell activation during the sensitization phase in contact hypersensitivity. Int Immunol 2001;13:1471–8.
[31] Imai S, Atarashi K, Ikesue K, Akiyama K, Tokura Y. Establishment of murine model of allergic photocontact dermatitis to ketoprofen and characterization of pathogenic T cells. J Dermatol Sci 2006;41:127–36.
[32] Tokura Y, Yagi J, O'Malley M, Lewis JM, Takigawa M. Superantigenic staphylococcal exotoxins induce T-cell proliferation in the presence of Langerhans cells or class II-bearing keratinocytes and stimulate keratinocytes to produce T-cell-activating cytokines. J Invest Dermatol 1994;102: 31–8.
[33] Livak KJ, Schmittgen TD. Analysis of relative gene expression data using real-time quantitative PCR and the 2(−Delta Delta C(T)) method. Methods 2001;25:402–8.
[34] Okamoto H, Kripke ML. Effector and suppressor circuits of the immune response are activated in vivo by different mechanisms. Proc Natl Acad Sci 1987;84:3841–5.
[35] Hauser C, Elbe A, Stingle G. The Langerhans cell. In: Goldsmith LA, editor. Physiology, biochemistry, and molecular biology of the skin. 2nd ed., New York, NY: Oxford University Press; 1991. pp. 1144–1163.
[36] Kabashima K, Sakata D, Nagamachi M, Miyachi Y, Inaba K, Narumiya S. Prostaglandin E2–EP4 signaling initiates skin immune responses by promoting migration and maturation of Langerhans cells. Nat Med 2003;9:744–9.

DOI 10.1111/j.1365-2133.2007.07774.x

Inhibition of T helper 2 chemokine production by narrowband ultraviolet B in cultured keratinocytes

R. Hino, M. Kobayashi, T. Mori, H. Orimo, T. Shimauchi, K. Kabashima and Y. Tokura

Department of Dermatology, University of Occupational and Environmental Health, Kitakyushu, Fukuoka 807-8555, Japan

Correspondence
Ryosuke Hino.
E-mail: hinoti@med.uoeh-u.ac.jp

Accepted for publication
15 October 2006

Key words
chemokine, cytokine, keratinocyte, ultraviolet B

Conflicts of interest
None declared.

Summary

Background Narrowband ultraviolet B (NB-UVB) has recently been used for the treatment of various skin disorders. Its effects on the production of cytokines and chemokines by keratinocytes are unknown.

Objectives To investigate the effect of NB-UVB on production of chemokines and proinflammatory cytokines by keratinocytes in comparison with broadband (BB)-UVB.

Methods Normal human epidermal keratinocytes (or the human keratinocyte cell line HaCaT in some experiments) at semiconfluency were irradiated with NB-UVB at 10, 100, 500 or 1000 mJ cm^{-2} or BB-UVB at 10 or 100 mJ cm^{-2}. The cultures were maintained in the presence or absence of interferon (IFN)-γ at 200 U mL^{-1}. The 72-h culture supernatants were analysed by enzyme-linked immunosorbent assay to quantify T helper (Th)1 chemokines (IFN-inducible protein 10 and monokine induced by IFN-γ), Th2 chemokines [macrophage-derived chemokine (MDC) and thymus and activation-regulated chemokine (TARC)] and proinflammatory cytokines [interleukin (IL)-1α and tumour necrosis factor (TNF)-α]. The expression of mRNA for these molecules was simultaneously assessed by reverse transcriptase-polymerase chain reaction. The culture supernatants were also tested for their chemotactic activity for Th1 and Th2 cells. The two UVB sources were compared on the basis of their minimal erythemal doses and clinically used doses.

Results Although both NB-UVB and BB-UVB increased the production of IL-1α and TNF-α, the augmentative effect of NB-UVB was less than that of BB-UVB. Both wavelength ranges of UVB enhanced or had no effect on Th1 chemokine production, but suppressed the production of Th2 chemokines MDC and TARC. This was confirmed by chemotactic assay, which showed decreased chemotactic activity for Th2 cells by the culture supernatants from NB-UVB-irradiated keratinocytes.

Conclusions NB-UVB reduces the production of Th2 chemokines without excess production of proinflammatory cytokines, suggesting its therapeutic effectiveness on Th2-mediated skin disorders as well as its relative safety in clinical usage.

Ultraviolet B (UVB) radiation has been used for the treatment of various skin diseases. As compared with psoralen UVA (PUVA) photochemotherapy, UVB phototherapy has an advantage in daily clinical use because it is not necessary to administer psoralen. Parrish and Jaenicke[1] reported that UVB of wavelength 313 nm is most effective for the treatment of psoriasis. This finding provided the impetus for developing the Philips TL-01 fluorescent bulb, the narrowband (NB)-UVB radiation source, which produces a spectral emission at 310–315 nm. NB-UVB phototherapy has thus significantly improved the therapeutic efficacy of conventional broadband (BB)-UVB (290–320 nm) phototherapy for skin diseases such as psoriasis, atopic dermatitis, vitiligo and others.[2–7] Although a study in mice indicated that NB-UVB induced more skin cancers than BB-UVB therapy,[8] we have found that NB-UVB yields less oxidative DNA damage than BB-UVB when compared at clinically used doses.[9] In addition, the carcinogenic potential of NB-UVB is judged to be substantially lower than that of PUVA therapy.[10,11]

Keratinocytes are one of the major targets of UVB phototherapy. UVB irradiation induces not only the formation of DNA damage such as cyclobutane pyrimidine dimers in

keratinocytes but also the modulation of their immunological functions. The production of cytokines and the expression of adhesion molecules are profoundly changed by UVB in keratinocytes.[12–14] Although these alterations are concerned with the therapeutic effectiveness of UVB, the augmented production of proinflammatory cytokines, such as interleukin (IL)-1α and tumour necrosis factor (TNF)-α, may induce skin inflammation as an adverse effect. Therefore, it is of importance to compare the effect of NB-UVB with that of BB-UVB on the production of proinflammatory cytokines. There have been two reports regarding the modulatory effects of NB-UVB on cytokine production. In one study, whole-body NB-UVB irradiation did not alter the levels of immunomodulatory cytokines in the serum of human volunteers.[15] However, because cytokine modulation was assessed by serum concentration in this study, detection of changes occurring in the skin appears to be difficult. The other study demonstrated that NB-UVB irradiation decreased the production of proinflammatory cytokines by stimulated T cells.[16] No published study to date has analysed the effect of NB-UVB on cytokine and chemokine production by keratinocytes.

Recent accumulated findings have revealed that cell migration driven by the interaction between chemokines and chemokine receptors is pivotal in the pathogenesis of various inflammatory disorders.[17] In the skin, external stimuli or cytokines such as interferon (IFN)-γ and TNF-α[18] stimulate keratinocytes to produce various chemokines, which initiate migration of T cells and polymorphonuclear leucocytes. Among chemokines, macrophage-derived chemokine (MDC/CCL22) and thymus and activation-regulated chemokine (TARC/CCL17) are known as T helper (Th)2 chemokines that bind to CC chemokine receptor 4 (CCR4) on Th2 cells, whereas monokine induced by IFN-γ (MIG/CXCL9) and IFN-inducible protein 10 (IP-10/CXCL10) are Th1 chemokines with affinity for CXC chemokine receptor 3 (CXCR3) on Th1 cells.[19]

In this study, we compared NB-UVB and BB-UVB in their modulatory effects on the production of proinflammatory cytokines and Th1 and Th2 chemokines. Results suggest that both wavelength ranges of UVB similarly alter the production of these cytokines and chemokines, but the levels of modulation are different between them. Preferential downmodulation of Th2 chemokines by NB-UVB is especially interesting.

Materials and methods

Cell culture

Normal human epidermal keratinocyte (NHEK) cells isolated from neonatal foreskin were grown in the serum-free keratinocyte growth medium KGM-2 (Clonetics, San Diego, CA, U.S.A.), and subcultured using trypsin–ethylenediamine tetraacetic acid (Clonetics). Hydrocortisone was omitted 48 h before experiments. Cells of the human keratinocyte cell line HaCaT[20] were grown in Dulbecco's modified Eagle's medium (DMEM; Gibco-BRL Life Technologies Inc., Gaithersburg, MD, U.S.A.) supplemented with 10% heat-inactivated fetal calf serum (FCS), 100 U mL^{-1} penicillin and 100 μg mL^{-1} streptomycin (all from Gibco-BRL Life Technologies Inc.).

Ultraviolet B irradiation

Semiconfluent keratinocytes at third passage were obtained in six-well plates (Corning Glass Works, Corning, NY, U.S.A.) by plating the same number of keratinocytes. They were washed twice with 2 mL of phosphate-buffered saline (PBS; pH 7·4) and left in 300 μL of PBS. Cells were immediately irradiated with BB-UVB (FL-20 bulbs, emission range 280–340 nm, 305 nm max.; Toshiba-Medical Systems Corp., Tokyo, Japan) or NB-UVB (UV801 KL; Waldmann Medical Division, Villingen-Schwenningen, Germany; equipped with Philips TL-20W/01RS NB-UVB tubes; Philips, Eindhoven, The Netherlands).

The minimal erythema dose (MED) of BB-UVB is 50–150 mJ cm^{-2}, whereas that of NB-UVB is 500–1200 mJ cm^{-2}. The clinically used doses for patients with psoriasis vulgaris or mycosis fungoides of BB-UVB and NB-UVB are 50–300 mJ cm^{-2} and 300–1500 mJ cm^{-2}, respectively.[3,4,21] Thus, 8- to 10-fold higher doses of NB-UVB are clinically equivalent to BB-UVB.[9] Therefore, to evaluate and compare the effects of NB-UVB and BB-UVB on keratinocytes, we chose the irradiation doses of 10 and 100 mJ cm^{-2} for BB-UVB, and 100 and 1000 mJ cm^{-2} for NB-UVB. In some experiments, cells were exposed to NB-UVB at varying doses of 10, 50, 100, 500 and 1000 mJ cm^{-2} to see its maximal effect.

Immediately after UVB irradiation, PBS was replaced by DMEM in the presence or absence of 200 U mL^{-1} of recombinant human IFN-γ (Biogamma; Maruho Co., Osaka, Japan).

Quantification of cytokines and chemokines in culture supernatants

Three-day culture supernatants from NHEK and HaCaT cells were collected, stored at −70 °C, and measured for IL-1α, TNF-α, MDC, TARC, MIG and IP-10 by enzyme-linked immunosorbent assay (Genzyme-Techne, Minneapolis, MN, U.S.A.) according to the manufacturer's instructions. Optical density was measured with microplate reader Immuno-Mini NJ-2300 (Nihon InterMed, Tokyo, Japan).

Reverse transcriptase-polymerase chain reaction of mRNA for cytokines and chemokines

NHEK and HaCaT cells treated or untreated with UVB were incubated for 2 h in the presence or absence of 200 U mL^{-1} IFN-γ. Total RNA was isolated from cells using the SV Total RNA Isolation System (Promega, Madison, WI, U.S.A.). Reverse transcriptase-polymerase chain reaction (RT-PCR) was performed using the SuperScript First-Strand Synthesis System (Invitrogen, San Diego, CA, U.S.A.) according to the manufacturer's instructions. IL-1α, TNF-α, MDC, MIG and β-actin were amplified for 35 cycles, which achieved linear amplifica-

tion. The primers for human MDC have been described previously.[18] The other primers were as follows: IL-1α, 5′-TTGAGTTTAAGCCAT-3′ and 5′-GCATCATCCTTTGATG-ACTT-3′; TNF-α, 5′-CCTTGGTCTGGTAGGAGACG-3′ and 5′-CAGAGGGAAGAGTTCCCCAG-3′; MIG, 5′-TTAAACAATTTG-CCCCAAGC-3′ and 5′-CTGTTGTGAGTGGGATGTGG-3′; β-actin, 5′-GGCACCACACCTTCTACAATGAG-3′ and 5′-CGTCATACTCC-TGCTTGCTGACT-3′. PCR products were visualized on 1·5% agarose gels containing ethidium bromide.

Preparation of T helper (Th)1 and Th2 cells

Th1 and Th2 cells were established according to a previously reported method.[22] Briefly, for Th1-polarized cells, peripheral blood mononuclear cells (PBMC) from a normal subject were stimulated with anti-CD3 (Pharmingen, San Diego, CA, U.S.A.) and anti-CD28 (Immunotech SA, Marseille, France) monoclonal antibodies (mAbs) in 24-well plates (Corning Glass Works) for 3 days in the presence of recombinant IL-12, IL-2 (R&D Systems, Minneapolis, MN, U.S.A.) and anti-IL-4 mAb (Pharmingen) in RPMI-1640 (Gibco-BRL Life Technologies Inc., Grand Island, NY, U.S.A.) supplemented with 10% heat-inactivated FCS, 2 mmol L^{-1} L-glutamine, 5×10^{-5} mol L^{-1} 2-mercapto-ethanol, 10^{-5} mol L^{-1} sodium pyruvate, 25 mmol L^{-1} HEPES, 1% nonessential amino acids, 100 U mL^{-1} penicillin and 100 μg mL^{-1} streptomycin (all from Gibco-BRL Life Technologies Inc.). The culture was maintained for 3 weeks with the same cytokines and mAbs. Half medium change was performed once a week. For Th2-polarized cells, PBMC were stimulated with anti-CD3 and anti-CD28 mAbs and maintained in the presence of IL-4 (R&D Systems), IL-2, anti-IFN-γ mAb (BioSource International, Camarillo, CA, U.S.A.) and anti-IL-10 mAb (BioSource International).

Chemotaxis assay

PBMC were plated in Transwell inserts with a pore size of 5 μm and a diameter of 6·5 mm in 24-well plates (3421; Costar, Corning Life Sciences, Acton, MA, U.S.A.). PBMC (2×10^6) in 100 μL were added to the upper wells and 590 μL of culture supernatant was placed in the bottom wells, and plates were incubated for 3 h at 37 °C in 5% CO_2. To determine Th1 and Th2 subsets of migrating cells, cells that moved to the lower chamber were stained with mAbs directed against chemokine receptors: CXCR3 expressed on Th1 cells and CCR4 on Th2 cells. The cells were double stained with fluorescein isothiocyanate (FITC)-labelled anti-CD4 mAb and phycoerythrin (PE)-labelled anti-CXCR3 or anti-CCR4 mAb (BD Biosciences Pharmingen, San Diego, CA, U.S.A.) and analysed on a FACSCalibur (BD Biosciences Pharmingen).[18] Either FITC-labelled mouse IgG1 or PE-labelled mouse IgG1 was used as an isotype-matched control. Duplicate wells were analysed for each condition. Data were expressed as % input, which indicates [(the number of migrating cells)/(the number of applied cells)] × 100. Th1 and Th2 cells were also used as migratory cells.

Statistical analysis

Student's *t*-test was employed to determine the difference between means; $P < 0{\cdot}05$ was considered to be significant.

Results

Background study

It is well known that production of proinflammatory cytokines IL-1α and TNF-α by keratinocytes is enhanced by BB-UVB.[12–14] However, our preliminary study showed that the production of chemokines was differentially modulated by UVB, as MIG was enhanced, MDC and TARC were suppressed, and IP-10 was unchanged or slightly increased by BB-UVB. To evaluate the effect of UVB on each chemokine using the same experimental system, we therefore cultured UVB-irradiated NHEK cells in the presence (Figs 1–6) or absence (Table 1) of 200 U mL^{-1} IFN-γ in the experiments described below. When UVB suppressed the production of a given chemokine, this IFN-γ-augmented system was helpful to assess its suppressive effect clearly. Inversely, even when UVB increased the production of a given chemokine, UVB enhancement was detected in the nonstimulated condition and could also still be observed in the IFN-γ-stimulated condition.

Cell viability, as assessed by trypan blue dye exclusion test, was kept at 92–95% in NHEK cells treated with NB-UVB at 100 or 1000 mJ cm^{-2}, or with BB-UVB at 10 or 100 mJ cm^{-2}.

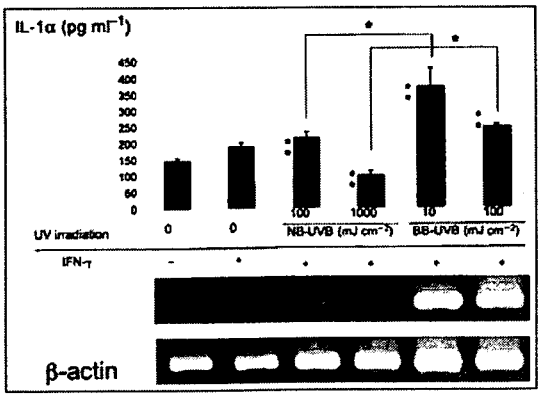

Fig 1. Interleukin (IL)-1α production and expression by normal human epidermal keratinocyte (NHEK) cells irradiated with ultraviolet B (UVB). NHEK cells were irradiated with narrowband (NB)- or broadband (BB)-UVB at the indicated dose and cultured in the presence or absence of interferon (IFN)-γ at 200 U mL^{-1}. The concentration was measured by enzyme-linked immunosorbent assay in 3-day culture supernatants. The expression of mRNA was analysed by reverse transcriptase-polymerase chain reaction. Data are expressed as means ± SD of triplicate cultures. *$P < 0{\cdot}05$, between the means. **$P < 0{\cdot}05$, compared with no UV with IFN-γ.

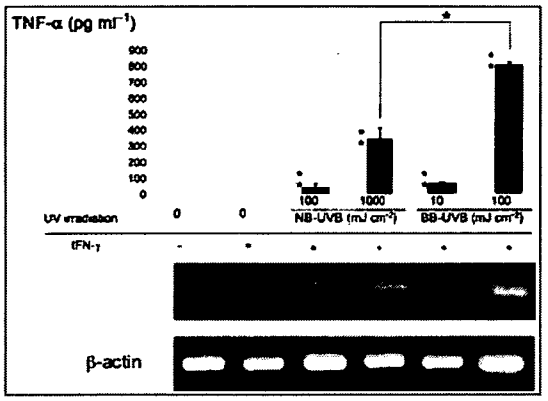

Fig 2. Tumour necrosis factor (TNF)-α production and expression by normal human epidermal keratinocyte cells irradiated with narrowband ultraviolet B (NB-UVB) or broadband (BB)-UVB. See Fig. 1 legend for details. *P < 0·01, between the means. **P < 0·05, compared with no UV with interferon (IFN)-γ.

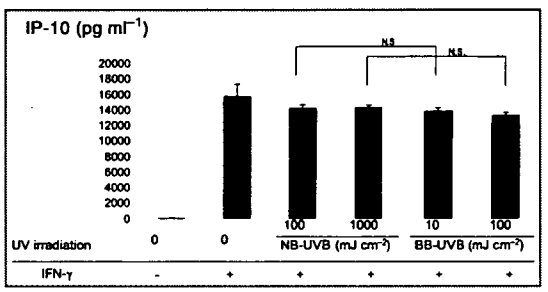

Fig 3. Interferon (IFN)-inducible protein 10 (IP-10) production by normal human epidermal keratinocyte cells irradiated with narrowband ultraviolet B (NB-UVB) or broadband (BB)-UVB. See Fig. 1 legend for details. N.S., not significant.

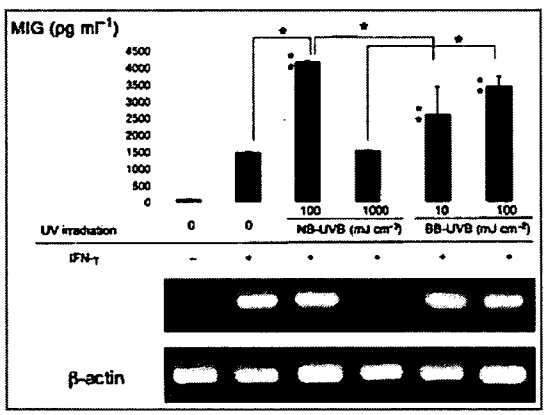

Fig 4. Monokine induced by interferon (IFN)-γ (MIG) production and expression by normal human epidermal keratinocyte cells irradiated with narrowband ultraviolet B (NB-UVB) or broadband (BB)-UVB. See Fig. 1 legend for details. *P < 0·05, between the means. **P < 0·05, compared with no UV with IFN-γ.

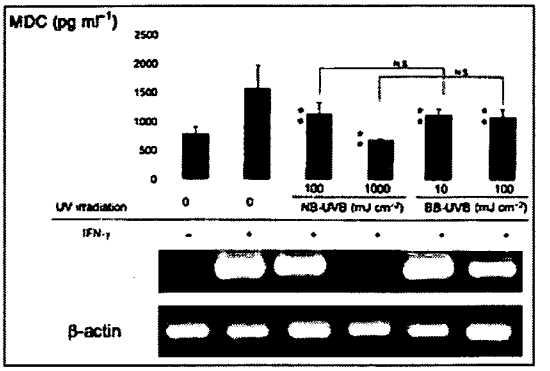

Fig 5. Macrophage-derived chemokine (MDC) production and expression by normal human epidermal keratinocyte cells irradiated with narrowband ultraviolet B (NB-UVB) or broadband (BB)-UVB. See Fig. 1 legend for details. N.S., not significant. **P < 0·05, compared with no UV with interferon (IFN)-γ.

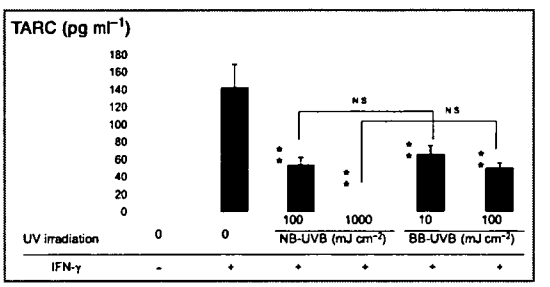

Fig 6. Thymus and activation-regulated chemokine (TARC) production by HaCaT cells irradiated with narrowband ultraviolet B (NB-UVB) or broadband (BB)-UVB. See Fig. 1 legend for details. N.S., not significant. **P < 0·05, compared with no UV with IFN-γ.

Less augmentative effects of narrowband ultraviolet B (NB-UVB) than broadband (BB)-UVB on proinflammatory cytokine production

We first examined the effect of two sources of UVB on the production of proinflammatory cytokines. Both NB-UVB and BB-UVB significantly augmented the production of IL-1α in the presence (Fig. 1) or absence (Table 1) of IFN-γ. The most augmentative dose of NB-UVB was 50–100 mJ cm^{-2} (data not shown). Considering that 8- to 10-fold higher doses of NB-UVB are equivalent to BB-UVB in the MED and in clinical use, the enhanced degree of IL-1α production by BB-UVB was higher than that by NB-UVB at both protein and mRNA levels.

More pronouncedly, the production and expression of TNF-α was promoted by both NB-UVB and BB-UVB (Fig. 2, Table 1). As 1000 mJ cm^{-2} NB-UVB and 100 mJ cm^{-2} BB-UVB were more augmentative than 100 and 10 mJ cm^{-2}, respectively, high doses of UVB were more effective for the increment of TNF-α than of IL-1α. Likewise, TNF-α was produced more effectively by BB-UVB than by NB-UVB. Thus, NB-UVB was less augmentative than BB-UVB in the production of proinflammatory cytokines.

Table 1 Percentage augmentation of cytokine and chemokine production by narrowband ultraviolet B (UVB) or broadband UVB in keratinocytes unstimulated with interferon-γ

	Control (pg mL^{-1})[a]	NB-UVB[b] 100 mJ cm^{-2}	NB-UVB[b] 1000 mJ cm^{-2}	BB-UVB[b] 10 mJ cm^{-2}	BB-UVB[b] 100 mJ cm^{-2}
IL-1α	144	49%	−32%	90%	42%
TNF-α[c]	<Detection	39 pg mL^{-1}	317 pg mL^{-1}	52 pg mL^{-1}	726 pg mL^{-1}
MIG	85	59%	−31%	−6%	8%
IP-10	24	92%	59%	279%	−27%
MDC	784	−55%	−52%	−54%	−69%
TARC	<Detection	<Detection	<Detection	<Detection	<Detection

NB-UVB, narrowband ultraviolet B; BB-UVB, broadband ultraviolet B; IL-1α, interleukin 1α; TNF-α, tumour necrosis factor-α; MIG, monokine induced by interferon (IFN)-γ; IP-10, IFN-inducible protein 10; MDC, macrophage-derived chemokine; TARC, thymus and activation-regulated chemokine. Normal human epidermal keratinocyte cells (for IL-1α, TNF-α, MIG, IP-10 and MDC) and HaCaT cells (for TARC) were irradiated with NB-UVB at 100 or 1000 mJ cm^{-2}, or with BB-UVB at 10 or 100 mJ cm^{-2}, and cultured in triplicate for 3 days in the absence of IFN-γ. The culture supernatants were analysed by enzyme-linked immunosorbent assay to quantify the indicated cytokines and chemokines. [a]The control values represent the mean concentration (pg mL^{-1}) of cytokines and chemokines in nonirradiated keratinocytes. [b]The values in the irradiated groups are expressed as the mean percentage augmentation: [(irradiated group−control group)/control group] ×100. [c]As the control level of TNF-α is under the level of detection, the absolute concentrations (pg mL^{-1}) are shown.

Suppression of T helper 2 chemokine production by narrowband ultraviolet B (NB-UVB) and broadband (BB)-UVB

We explored the effects of UVB on keratinocyte production of Th1 chemokines IP-10 and MIG, and Th2 chemokines MDC and TARC. Production of these chemokines was assessed in NHEK cells; however, because NHEK cells are incapable of producing TARC in the known culture conditions,[23] the production of this chemokine was assessed in HaCaT cells.

In the presence of IFN-γ, IP-10 production was not significantly affected at any dose of either NB-UVB or BB-UVB (Fig. 3), whereas its production was enhanced by both UVB sources in the absence of IFN-γ (Table 1). MIG production was increased by both NB-UVB and BB-UVB under IFN-γ-stimulated conditions (Fig. 4).

MDC production was suppressed by both NB-UVB and BB-UVB (Fig. 5, Table 1). At the lower doses, the two UVB sources produced comparable suppression. Similarly, in HaCaT cells, both UVB ranges at the lower doses profoundly suppressed TARC production at comparable levels (Fig. 6). The higher dose of NB-UVB exerted a markedly stronger inhibitory effect.

These results demonstrate that both NB-UVB and BB-UVB downmodulate the production of Th2 chemokines but not Th1 chemokines. The suppressive activity of NB-UVB was rather stronger than BB-UVB.

Chemotactic responses of T helper (Th)1 and Th2 cells to keratinocyte culture supernatants

We examined the biological chemotactic activity of culture supernatants from NHEK cells irradiated with NB-UVB or BB-UVB. PBMC were incubated in the upper Transwell chamber for 3 h, and the numbers of CXCR3 Th1 and CCR4 Th2 cells that migrated to keratinocyte supernatants were enumerated using flow cytometry (Fig. 7). The chemotactic response of both CXCR3+ Th1 and CCR4+ Th2 cells to the supernatant was enhanced by IFN-γ treatment of NHEK cells (Fig. 8). NB-UVB irradiation of NHEK cells at 100 mJ cm^{-2} before culture with IFN-γ profoundly suppressed the Th2 chemotactic activity of supernatants, whereas the Th1 chemotactic activity was rather enhanced by this dose of NB-UVB. The higher dose (1000 mJ cm^{-2}) of NB-UVB suppressed production of both Th1 and Th2 chemokines. BB-UVB also suppressed Th2 chemokines more markedly than Th1 chemokines, but its suppressive ability for Th2 chemokines was slightly lower than that of NB-UVB. Virtually the same chemotactic activities of the supernatants were found in the migratory study using Th1- and Th2-polarized cells as responders (Fig. 9). These data confirm that exposure of keratinocytes to NB-UVB suppresses their production of Th2 chemokines.

Discussion

Our study demonstrated that UVB differentially modulates the production of each cytokine or chemokine by keratinocytes. Similar to BB-UVB, which is well known to augment the production of IL-1α and TNF-α,[12–14] NB-UVB also increased the proinflammatory cytokines but to lesser degrees. More interestingly, both UVB sources altered the production of chemokines at the doses stimulatory for these proinflammatory cytokines. Whereas Th1 chemokines were augmented by UVB, MDC and TARC were depressed by ~60% at the doses tested, suggesting that Th2 chemokines are preferentially downmodulated by UVB as compared with Th1 chemokines and proinflammatory cytokines. This Th2 chemokine-dominant suppression was confirmed by the chemotaxis assay, which showed that the culture supernatants from keratinocytes irradiated with UVB, in particular NB-UVB, had low chemotactic activity for Th2 cells.

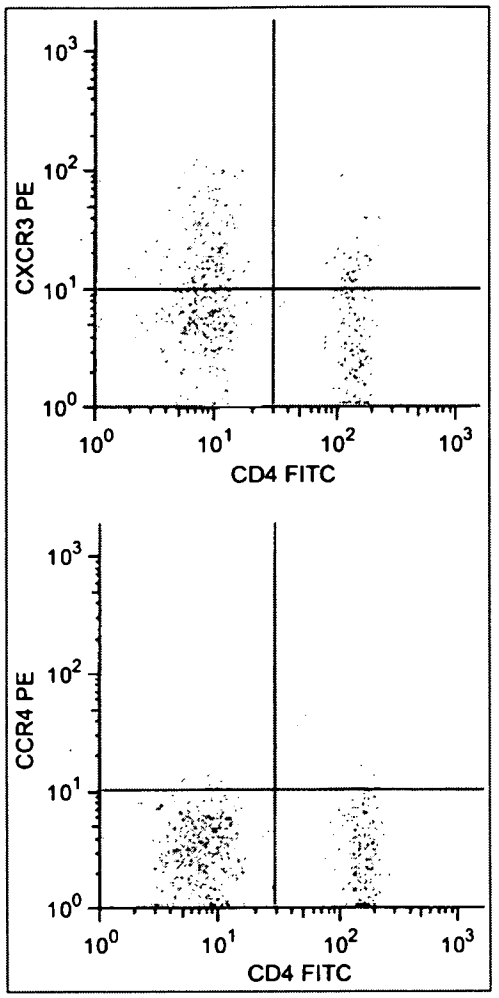

Fig 7. Flow cytometric analysis of migrating T helper (Th)1 and Th2 cells. Peripheral blood mononuclear cells from a normal subject were applied to the Transwell chamber. The migrating cells were subjected to flow cytometric analysis. Th1 and Th2 cells were identified as cells positive for CD4/CXC chemokine receptor 3 (CXCR3) and CD4/CC chemokine receptor 4 (CCR4), respectively. The panels show representative data, which were obtained from HaCaT cell supernatants of 100 mJ cm^{-2} narrowband ultraviolet B for Th1 cells and those of interferon-γ treatment alone for Th2 cells. FITC, fluorescein isothiocyanate; PE, phycoerythrin.

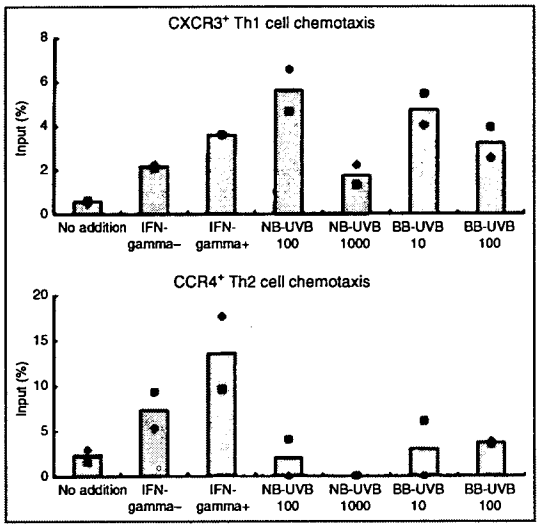

Fig 8. T-cell chemotactic activity of keratinocyte supernatants treated with narrowband ultraviolet B (NB-UVB) or broadband (BB)-UVB. Results are expressed as the percentage of input cells of each subtype migrating to the lower chamber of a Transwell filter containing culture supernatants from keratinocytes treated with or without interferon (IFN)-γ (200 U mL^{-1}), NB-UVB (100 or 1000 mJ cm^{-2}), or BB-UVB (10 or 100 mJ cm^{-2}) irradiation. Panels show migration of peripheral blood mononuclear cell subsets: CXC chemokine receptor 3 (CXCR3)+ T helper (Th)1 cells and CC chemokine receptor 4 (CCR4)+ Th2 cells. Diamonds and squares represent the numerical values of % input.

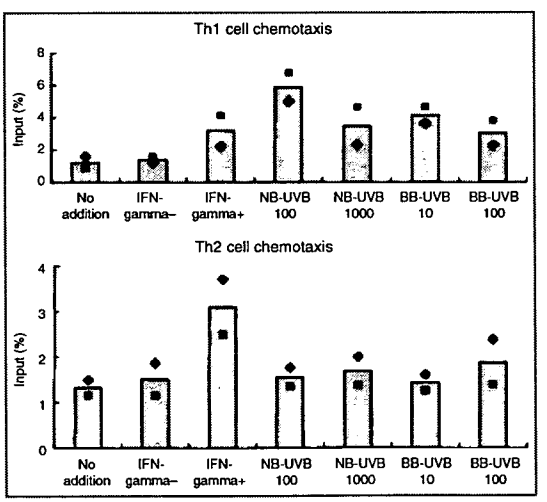

Fig 9. T helper (Th)1- and Th2-cell chemotactic activity of keratinocyte supernatants treated with narrowband ultraviolet B (NB-UVB) or broadband (BB)-UVB. Th1- and Th2-polarized cells were cultured from peripheral blood mononuclear cells from a normal subject with different combinations of cytokines and anticytokine monoclonal antibodies. Results are expressed as described in Fig. 8. Panels show migration of Th1 cells and Th2 cells.

In general, the production of the four chemokines tested here can be stimulated with IFN-γ, or more effectively with the combination of IFN-γ and TNF-α.[18,23] Although we used IFN-γ alone as a stimulant, TNF-α secreted from UVB-irradiated keratinocytes was considered to cooperate with IFN-γ in chemokine production. It seemed that UVB modulated the chemokine production as a combined result of its direct and indirect TNF-α-mediated effects. Additionally, it is possible that MIG was elevated by UVB as a consequence of the